

Optical imaging techniques for hypersonic impulse facilities

T. J. McIntyre

School of Physical Sciences, The University of Queensland
Brisbane
Australia

H. Kleine

School of Aerospace, Civil & Mechanical Engineering,
University of New South Wales, Australian Defence Force Academy
Canberra
Australia

A. F. P. Houwing

Department of Physics and Theoretical Physics, Australian National University
Canberra
Australia

ABSTRACT

The application of optical imaging techniques to hypersonic facilities is discussed and examples of experimental measurements are provided. Traditional Schlieren and shadowgraph techniques still remain as inexpensive and easy to use flow visualisation techniques. With the advent of faster cameras, these methods are becoming increasingly important for time-resolved high-speed imaging. Interferometry's quantitative nature is regularly used to obtain density information about hypersonic flows. Recent developments have seen an extension of the types of flows that can be imaged and the measurement of other flow parameters such as ionisation level. Planar laser induced fluorescence has been used to visualise complex flows and to measure such quantities as temperature and velocity. Future directions for optical imaging are discussed.

NOMENCLATURE

A	effective rate for spontaneous emission
A_{las}	cross-sectional area of the laser sheet
B	Einstein coefficient for absorption
c	speed of light
C_{opt}	efficiency of the optical system
e	charge on an electron
E	laser energy
f	oscillator strength
f_B	Boltzmann fraction of the absorbing state

g	spectral overlap integral
G	Gladstone-Dale coefficient
k	Boltzmann constant
K	numerical constant ($4.48 \times 10^{-16} \text{m}$)
l	path length of light through a flow
m	mass
n	refractive index
N	species number density
p	fringe shift
P	pressure
Q	collisional quenching rate
S	fluorescence signal
T	temperature
ϵ	permittivity
λ	wavelength of light
ρ	density
ϕ	phase of a light wave
Φ	fluorescence yield
χ	mole fraction

Subscripts

0	subscript indicating reference (usually free-stream) conditions
e	subscript referring to electrons
p	subscript referring to value per laser pulse
λ	subscript referring to quantity at a given wavelength

Paper No. 3128. Manuscript received 22 August 2006, accepted 7 December 2006.

This is the latest in a series of invited survey papers focusing on a specific aspect of the aeronautical industry.

1.0 INTRODUCTION

Optical imaging techniques have played a major role in the investigation of a wide variety of fluid flows. Their application ranges from providing high clarity qualitative images to the quantification of important fluid mechanical properties including density, temperature, pressure, velocity and species concentration. It is now routine to use such images for comparison with numerical simulations leading to a better understanding of the characteristics of the flow.

Optical techniques rely on the interaction of light with the gas molecules to change a given characteristic of the light such as its intensity, direction, wavelength, or phase. Classically, the interaction of light with a gas is described as the excitation of electric dipoles by the oscillating electrical field of the light. This process is described by the (complex) absorption coefficient which is dependent on characteristics of the gas itself and the frequency of the exciting light. The resultant scattering of the light can be categorised into an interaction with the real part of the refractive index through the absorption coefficient, or with the imaginary part of the refractive index which is given by the dispersion relation. At higher laser intensities, non-linear effects can also be present. A range of experimental schemes have been developed to make use of these interactions for flow imaging.

The purpose of this paper is to review current state-of-the-art imaging techniques that are applied to impulse facilities capable of generating chemically reacting hypersonic flows. The types of facilities under consideration include shock tubes and tunnels, expansion tubes, arc jets and vitiated facilities⁽¹⁾. The imaging techniques are broadly categorised into Schlieren and shadowgraph methods which rely on the deflection of light due to refractive index gradients, interferometric techniques using a change in the phase of the light as it propagates, and fluorescence techniques which image light emitted by laser-excited molecules in an illuminated region of the flow. The present review has a particular emphasis on shock tunnel studies and we present sample images generally from work completed by the authors. References are given to publications of many other groups. In restricting our review to imaging techniques in impulse facilities, we preclude discussion on a range of other optical techniques such as tunable diode laser absorption spectroscopy, coherent anti-Stokes Raman scattering, and polarisation spectroscopy. The latter techniques are either point-wise measurements, or are yet to be applied to high-speed impulse facilities of the type considered here.

2.0 SCHLIEREN AND SHADOWGRAPH

2.1 Overview

Since their inception in the 19th century, the density-sensitive Schlieren and shadowgraph techniques have been staple diagnostic tools for the investigation of compressible flows. In the second half of the 20th century, when hypersonic flow research commenced, these techniques had already matured so that it came as no surprise that they initially became the almost exclusive optical means for investigations of the structures of hypersonic flows. The specific challenges of the hypersonic flow environment, discussed further below, and the quest for more quantitative optical measurements have to some extent changed the role of Schlieren and shadowgraph visualisation into that of a supplementary diagnostic rather than the main tool for a thorough investigation. Laser-based visualisation diagnostics, which offer also the possibility to measure certain thermodynamic properties of the flow in addition to visualising its geometric structure, have matured over the last two decades, but they are unlikely to replace the Schlieren and shadowgraph methods. In the early stages of the development of the laser-based diagnostics, the results obtained were verified by simultaneous or additional Schlieren visualisation⁽²⁾ – a feature that is likely to remain. In

addition, Schlieren and shadowgraph techniques offer certain crucial advantages, which often compensate for the smaller amount of quantitative information they can deliver. The most obvious advantage is the robustness and relative simplicity of these systems, coupled with the fact that they are significantly more economical (a good Schlieren apparatus with a field of view up to 300mm diameter may be obtained for approximately US\$50,000, which is a small fraction of the price of more advanced optical systems). In addition, Schlieren and shadowgraph methods can quite easily be operated in time-resolved mode, provided an adequate light source/camera combination is available, and are thus an important tool when information on the time history of a hypersonic flow is required. Recent advances in digital high-speed video cameras have made this aspect particularly attractive. Finally, Schlieren images and shadowgrams provide arguably the most graphic representations of a flow-field, from which qualitative and phenomenological descriptions of the processes in a compressible flow can be obtained with relative ease. As these images are immediately available without the need for post-processing of extensive measurement records, the results allow the user of these techniques to evaluate an experiment with no or only minimum delay.

One further difference between Schlieren and shadowgraph methods and laser-based diagnostics is their historical relation to hypersonics. As indicated above, Schlieren and shadowgraph techniques had already been brought to a high level of maturity before they were used to investigate hypersonic flow-fields. As a consequence, the applied systems were only marginally modified and refined with respect to the apparatuses that had already been (and still are) used to visualise ‘normal’ supersonic flows. These modifications are related to the special conditions and challenges a hypersonic flow generates, but they usually do not alter the basic layout of the optical system. These special conditions and their consequences are discussed further below. On the other hand, many of the laser-based systems described in the later sections of this contribution have been specifically tailored and developed for an application in hypersonics. This difference between an established and almost universally applicable technique and specific newly developed custom-made methods becomes obvious in the list of references. While Schlieren and shadowgraph techniques have been extensively used in a large number of investigations of hypersonic flows, only few papers mention explicitly the modifications introduced in the optical system to make it useful for this task. On the other hand, a significantly larger portion of publications describe in greater detail the characteristics of special laser-based diagnostic techniques developed for an application in a hypersonic flow environment.

2.2 Density-sensitive flow visualisation

The theory and the variety of Schlieren and shadowgraph systems has been extensively described in a number of publications (e.g., Refs 3–5), so that only a brief outline of the underlying principles will be given here.

When a light beam traverses an area of varying density, it is displaced, deflected, and retarded or accelerated. In other words, it will reach a recording plane behind this area at a different location, under a different impingement angle, and at a different time. Density variations within a (transparent) flowing medium lead to these modifications of a traversing light beam – the recording of these modifications essentially then yields a picture of the flow. Strictly speaking, one does not take a picture of the flow itself but of the changes and disturbances it induces in an array of light beams⁽³⁾.

Each of the aforementioned modifications yields a different derivative of the density and each can be recorded exclusively by a particular set of corresponding techniques. The shadowgraph technique records the displacement of the light beam, which is proportional to the second derivative of the density. In a Schlieren system the angular deflection of the light beam is detected, that is,

the change of direction that this light beam experiences on its path through a medium of varying refractive index. This is a measure of the density gradient, that is, the first derivative. The retardation or acceleration of the light beam, measured by interferometry, is related to the density ρ itself.

The shadowgraph system provides the least complex apparatus, which in its simplest form only requires an approximately point-like light source and a recording screen, which is placed at a certain distance behind the flow (the position of this screen is often referred to as the 'shadow plane'). The discontinuities in the flow deflect the light, which leads to illumination variations on the recording screen – hence the flow casts a shadow^(3,5). For reasons outlined further below, this simplest visualisation arrangement is rarely used for hypersonic flows, but shadowgraph systems for this application often resemble a Schlieren set-up in which the knife edge has been removed and where the imaging optics focus on the shadow plane rather than on the flow itself^(4,5).

The principle of the Schlieren technique is to separate deflected from undeflected (that is, undisturbed) light beams. If the deflected beam is intercepted by an appropriate cutoff-device (for example, by a knife edge), the corresponding point in the test section, where the light deflection occurred, appears darker in the image plane. Similarly, one can reverse this system by blocking off undisturbed light beams and only admitting deflected ones to the screen, where corresponding image points of the test section would now appear brighter. In a monochrome system, density gradients are thus represented by changes of illumination^(3,5). Only deflections (and thus density gradients) normal to the cut-off device become visible this way.

The human eye is generally more sensitive to detect changes of hue rather than changes of illumination intensity. Therefore, it has been tried almost since the inception of these techniques to introduce colour to Schlieren systems. Initial versions of colour Schlieren apparatuses, either prism-based or with a set of coloured filters replacing the knife edge^(3,4), suffered from a strongly reduced image quality in the recording plane, caused by diffraction effects at the cut-off device. The dissection technique introduced by Cords⁽⁶⁾ eventually overcame these difficulties. Colour Schlieren techniques generally tend to be less sensitive than the monochrome methods, however, they provide a greater sensitivity range. By choosing a particular colour filter layout, the colours may be used as the carrier of information that would be difficult if not impossible to display by means of just changes of illumination: it is possible to show the direction of a density gradient, as opposed to its magnitude, which is recorded by the conventional knife edge methods^(4,5). This technique allows one to detect all gradients normal to the direction of light ray propagation. Therefore, in a plane flow all phenomena that alter the local fluid density are visualised. The photos obtained with the direction-indicating colour Schlieren technique are usually very clearly structured and thus most suitable for interpretation and phenomenological descriptions of the flow.

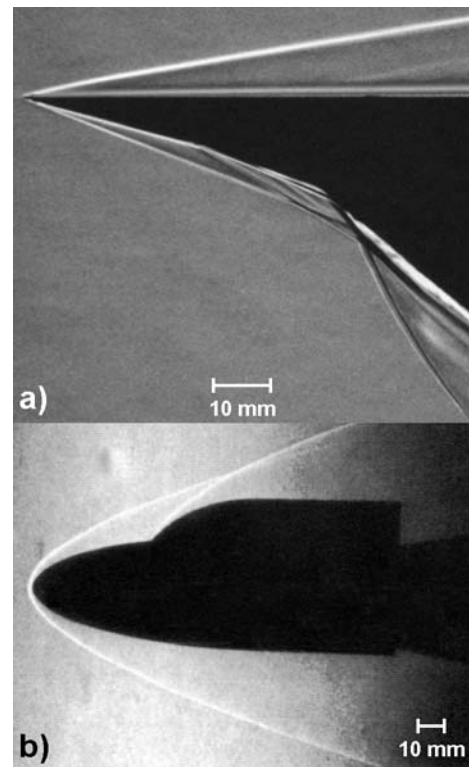


Figure 1. Schlieren visualizations of hypersonic flows; from⁽¹¹⁾
 a) flow over flat plate/wedge assembly, $M_x = 7.73$, $Re_x = 3.9 \times 10^6$ 1/m, $h_0 = 1.652$ MJ/kg; direction-indicating colour Schlieren;
 b) flow over double ellipsoid model, $M_x = 7.24$, $Re_x = 4.3 \times 10^6$ 1/m, $h_0 = 1.652$ MJ/kg; standard monochrome Schlieren with vertical knife edge; the Schlieren head in this test had a focal length of 2,000mm; the model used in this test is a scaled down version of the model shown in Fig. 2

Differential or shearing interferometry, albeit being an interferometric method, yields results that are often almost indistinguishable from Schlieren visualisations^(3,5). A variety of systems has been developed, especially at the French-German Research Institute of Saint-Louis (ISL), and has subsequently been extensively applied for hypersonic flow research⁽⁷⁾. In spite of the conceptual differences between these techniques and the Schlieren methods, their diagnostic potential and their results, as well as the challenges encountered for the visualisation of hypersonic flows, are very similar so that these techniques need not be treated separately.

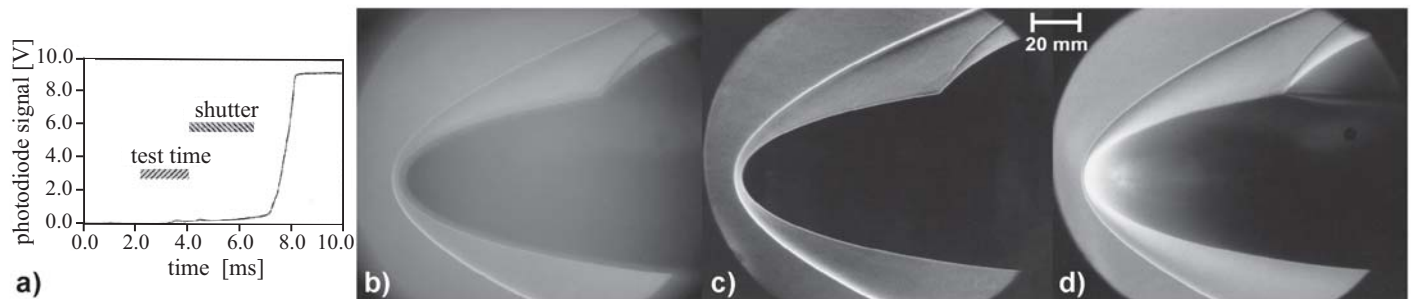


Figure 2. Effect of luminosity in the test section.

- a) luminosity as a function of time, with indication of useful test time and time required for electro-magnetic shutter to close optical path⁽¹²⁾.
- b) flow over double ellipsoid model, $M_x = 7.73$, $Re_x = 3.9 \times 10^6$ 1/m, $h_0 = 1.652$ MJ/kg; direction-indicating colour Schlieren; no shutter⁽¹²⁾.
- c) same model and flow condition as in (b), but with shutter; direction-indicating colour Schlieren⁽¹²⁾.
- d) same model as in (a), (b), but for $M_x = 6.13$, $Re_x = 3.6 \times 10^6$ 1/m, $h_0 = 6.838$ MJ/kg; direction-indicating colour Schlieren⁽¹¹⁾.

2.3 Challenges

Hypersonic flows are a challenging environment for flow visualisation. A number of different flow structures are often found within a small region in close proximity to the body immersed in the flow. Inviscid and viscous flow elements, for example, which in most other flows occupy physically distinct regions, often appear indistinguishably close to each other. In Fig. 1(a), the zone containing the leading shock coming from the tip of the wedge, the boundary layer developing on the wedge surface, another shock emanating from a change in wedge angle, and a small bubble of separated flow in front of a second (larger) wedge angle change is only about five millimetres wide, which is only a small fraction of the typical dimension of the model. The hues in the original colour image indicate also the presence of an entropy layer⁽⁸⁾. A meaningful visualisation of flow details therefore often requires an optical system that can provide images with high spatial resolution. This, in turn, makes high magnification optics and powerful short-duration light sources mandatory.

At the same time, in almost all ground-based test facilities the density level of the flow is inherently low, typically around or below one percent of the ambient density. This means that in spite of high density ratios across shocks and other discontinuities in hypersonic flows, the observed density changes and gradients are often minute. In fact, these low density levels, which severely limit the use of density-sensitive visualisation, were one of the main factors that have prompted the development of other optical techniques more suitable for the conditions in hypersonic flows. Most hypersonic blow-down or shock-tunnel facilities, however, generate flows that can be visualised with the help of Schlieren methods, but they require an appropriate Schlieren system with sufficient sensitivity. One advantage of Schlieren systems over interferometers is that the sensitivity can be controlled by the choice of the optical components⁽⁹⁾. For Schlieren systems, a high sensitivity can be achieved by using Schlieren heads with large focal lengths, which, however, can significantly increase the physical size of the optical system. In order to detect refraction angles of approximately one arc second typical Schlieren heads used in hypersonic facilities have focal lengths larger than 3,000mm. Should such a system (or the required space for it) not be available, the flow visualisation record is likely to depict only the major flow discontinuities (Fig. 1(b)). Bize *et al.*⁽¹⁰⁾ describe a system that can resolve a refraction as small as 0.01 arc seconds, specifically developed for the use in the ONERA La Fauga F4 Hotshot facility, where density levels can be as low as 10^{-6} g/m³. In shadowgraph systems, the sensitivity of the apparatus can be controlled by choosing the distance between the flow and the shadow plane, but an upper limit for this distance and therefore the sensitivity is imposed by an increasing blurring of the image⁽⁴⁾. For this reason, shadowgraph visualisation is only applied in facilities with comparatively high density levels.

Caused by the highly elevated thermodynamic states in hypersonic flows with temperatures of up to several thousand degrees, luminosity in the test section plays often an important – and mostly detrimental – role. Any light entering the optical system other than that of the probing beam, whose modifications are to be recorded, will influence and generally degrade the measurement result. Luminosity in the test section usually exists for a period significantly longer than the duration of the probing beam – the former is typically measured in milliseconds, the latter in microseconds. Therefore this light could reach the recording device before, during and after the instant the probing beam is generated. If the camera is not fully synchronised with the probing beam, even low levels of luminosity, applied over a longer time, can influence the flow visualisation. Unless one uses monochrome light sources and appropriate filters, light generated during the actual test time – normally from luminous areas in the stagnation zones of the body – cannot be prevented from reaching the recording material. As this light is generally highly divergent – in contrast to the collimated test beam – its effect can be mitigated by arranging the optical system in a way

that its components only receive and transmit a minimal portion of divergent light. Rigorous masking of mirrors and lenses as well as placing the components at large distances from the test section are possible remedies for this problem. The use of lasers as monochrome light sources, in conjunction with appropriate filters that block all wavelengths but that of the laser illumination, could be seen as a simpler solution (incidentally, most pulsed lasers would also be strong enough for a high-magnification visualisation), but such laser illumination is inferior to white light in a Schlieren system because of coherent artefact noise and diffraction problems at the knife edge and at the flow discontinuities themselves⁽⁴⁾. Luminosity in the test section is the main reason why simple contact shadowgraph – literally a photographic plate in contact with the test section window – is generally not a viable visualisation option for hypersonic flows.

The luminosity can have two sources, and depending on which one is dominant, there exist other solutions involving fast acting shutters and/or gated cameras. Any luminosity occurring during the actual test time and within the investigated flow-field can only be reduced by the aforementioned methods of filtering and appropriate arrangement and masking of all optical components. In some test facilities, however, the investigated flow itself is not the primary source of this luminosity. In all shock tunnels, the primary shock transmitted through the nozzle, which initiates the establishment of the hypersonic flow, eventually hits the end wall of the dump tank. Depending on the shock conditions and the geometry of the test section and dump tank, this reflection can be the main cause of luminosity. In the Aachen shock tunnel, for instance, a more than fifty-fold increase of luminosity was registered at a time that coincided with the arrival of the primary shock at the end wall of the dump tank (Fig. 2(a)). The light thus generated influenced the recorded Schlieren images for low enthalpy conditions (see Fig. 2(b)) but entirely obliterated the Schlieren signal for high enthalpy conditions. Due to the size of the dump tank (volume 19.2m³), the rapid increase in luminosity occurred approximately two to three milliseconds after the end of the test time, which left sufficient time for a specially developed electro-magnetic shutter to interrupt the light path at the location of the Schlieren cut-off^(11,12). Figures 2(b) to 2(d) illustrate the improvement of the visualisation that was achieved by introducing the fast acting shutter. The shutter also allowed one to use the more informative colour Schlieren technique instead of the inevitably monochrome recording methods that require filters to eliminate the effects of luminosity. A notable result from tests at higher enthalpy with more pronounced luminous zones around the test object is that these luminous zones can be significantly smaller than the actual shock layer (Fig. 2(d)).

While the development of such shutters was a technical solution pursued especially during the 1960s and 1970s (five contributions for various shutter designs can be found alone in the proceedings of the 8th and 9th International Congress on High-Speed Photography, 1968 and 1970), another way of obtaining ultra-short exposure times (and thus eliminating the recording of light emitted at any other instant but the specified moment of exposure) is to use electro-optical camera systems such as image converter cameras⁽¹³⁾. Early prototypes of image tubes with sub-microsecond exposure times were already available in the 1950s, but the focus of the development was time-resolved recording. Similar paths were followed in the development of high-speed charge coupled devices (CCD) and associated camera systems⁽¹⁴⁾. A number of commercial cameras of these types have become available over the last decades, but it appears that time-resolved recording is their primary application. Apart from the cost of these cameras, their limited spatial resolution is likely the main factor responsible for not having found widespread use in hypersonic flow research. In recent years, the initial complexity of the early versions of these camera types has given way to user-friendly compact devices, but limitations in resolution compared to regular film recordings are a perennial drawback of these systems.

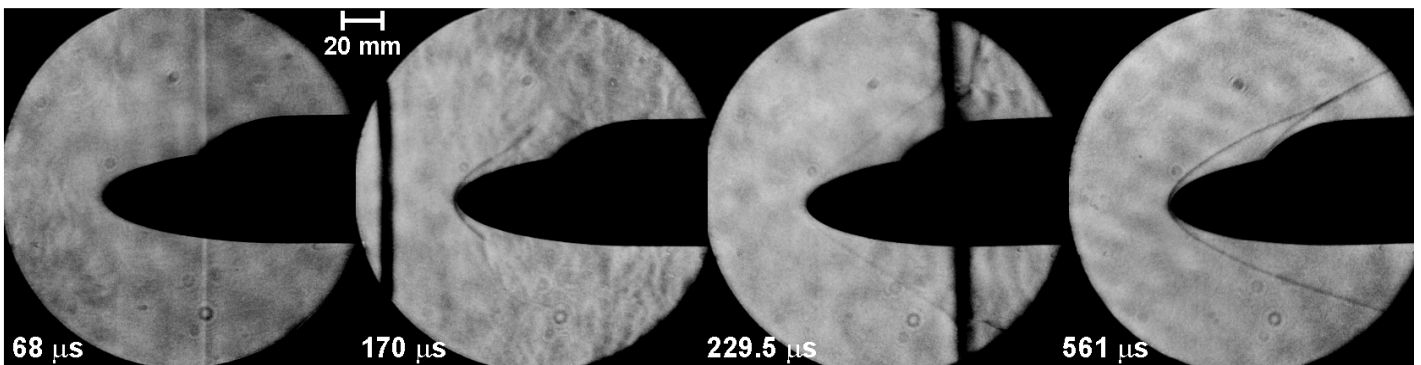


Figure 3. Time-resolved Schlieren visualisation of the starting process of a hypersonic flow ($M_\infty = 7.73$, $Re_\infty = 3.9 \times 10^6$ 1/m, $h_0 = 1.652$ MJ/kg); four frames of a sequence of 185 frames obtained with a ruby laser stroboscope and a rotating mirror camera at a frame rate of 117,650 fps: the initial shock transmitted through the nozzle (first frame; time is counted from the first appearance of the first shock in the test section) is followed by the considerably stronger second shock, which faces upstream but is washed downstream by the flow (second and third frame); the steady flow is generated after the passage of the second shock. Images courtesy of H. Olivier, Shock Wave Laboratory, RWTH Aachen.

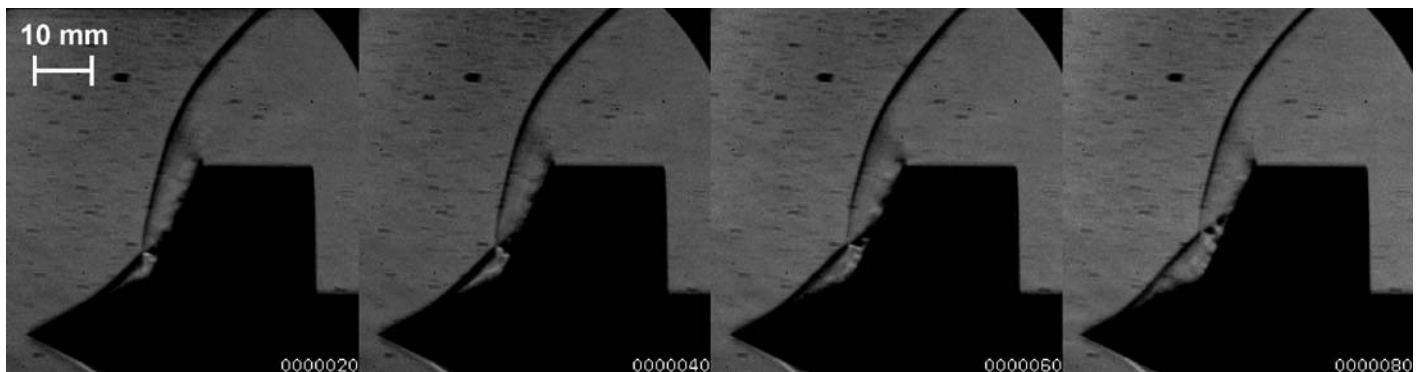


Figure 4. Time-resolved Schlieren visualisation of the unsteady hypersonic flow over a double cone (cone angles 50° and 130° ; $M_\infty = 6.99$, $Re_\infty = 3.5 \times 10^6$ 1/m, $h_0 = 4.8$ MJ/kg); four frames of a sequence of 100 frames obtained at 500,000fps with the high-speed video camera described in^(19,20); time interval between shown frames: $20\mu\text{s}$ ⁽¹⁵⁾.

2.4 Time-resolved visualisation

Time-resolved visualisation is a contentious issue for hypersonic ground facilities. Most of these facilities are characterised by an inherently short duration of useful test time, in which the flow is believed to be steady. Single-image visualisation has so far been justified by referring to the steady flow period, but most facilities determine this duration on the basis of probe measurements only (usually pressure or heat flux). The fact that two images, taken at slightly different instants in two separate tests run under the same initial conditions, normally show no marked difference has been used as an optical proof of the claimed steady flow test time. Given the complexity and the cost of tests in these facilities, only a few true optical verifications of the temporal characteristics of these facilities have been performed. It is anticipated that the future implementation of more readily available high-speed cameras is likely to clarify whether the claims regarding steady flow test time can be substantiated.

In addition to establishing whether or not a flow is truly steady, time-resolved visualisation enables one to investigate processes that are inherently unsteady, such as the starting process of the hypersonic flow (Fig. 3) or flow instabilities such as pulsations in the flow over a double cone (Figs 4⁽¹⁵⁾). One further advantage of time-resolved recording is that the aforementioned effects of luminosity play only a minor role as the recording medium (film or CCD) can only be accessed during a short period.

In contrast to most other visualisation methods, Schlieren and shadowgraph techniques can readily be used for time-resolved

visualisation if an appropriate light source – camera combination is available. Usually one combines either a stroboscopic light source with a continuously recording streak camera or a continuous light source with a framing camera. Numerous commercial systems as well as purpose-built laboratory-specific devices have been developed and used over the last seventy years.

Multiple spark sources such as those used with a Cranz-Schardin camera⁽¹⁶⁾ can obtain framing rates up to one MHz and generate between four and twenty-four images of single-shot quality. The spatial distribution of the spark sources, however, inevitably introduces a parallax that can be detrimental for a quantitative evaluation of the images.

Rotating mirror cameras⁽¹⁷⁾ offer usually a comparatively large number of frames with good to reasonable spatial resolution. Framing rate and exposure time cannot usually be varied during the recording.

Image converter cameras are very versatile and can easily generate more-than-sufficient framing rates approaching the GHz range^(13,18), but their internal optical arrangement causes an inevitable degradation of image resolution, which makes it often difficult to monitor the evolution of smaller flow elements. While the number of frames is limited (typically 8 to 16), recent models provide a convenient flexibility of framing rate and exposure time.

Only at the beginning of the new millennium have high-speed video systems started to become a serious alternative to the aforementioned high-speed cameras for observations in the MHz range. Earlier versions had even more obvious constraints with respect to image resolution and framing rate than all other available high-

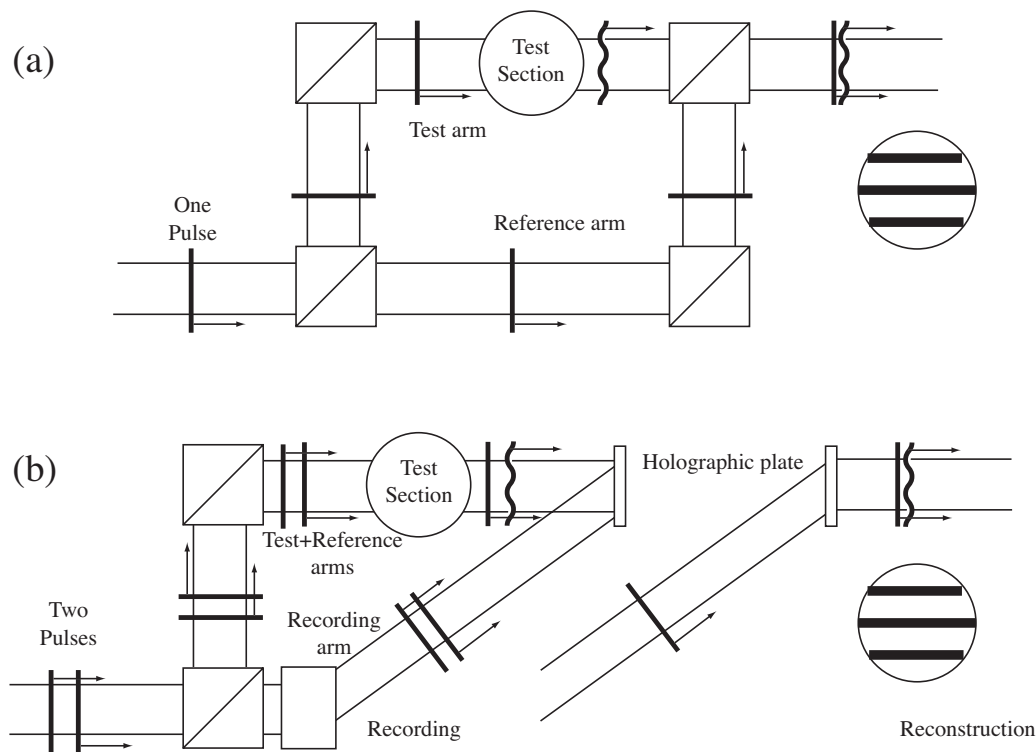


Figure 5

Figure 5. Schematic diagram of interferometry systems. (a) Mach-Zehnder Interferometry; (b) Holographic Interferometry.

speed photography apparatuses. Recent systems^(19,20), however, can record a sequence of one hundred images at framing rates of up to one million frames per second in full-frame mode. The obtained video images are marked by high resolution and outstanding quality⁽²⁰⁾. A similar high-speed camera, albeit with considerably lower resolution, and its application to hypersonic flow visualisation was described by Wu and Miles⁽²¹⁾. Further development and improvement of these cameras towards higher resolution, increased frame number and colour recording is currently being pursued^(22,23), and the increased use of these devices in hypersonic test facilities is likely to have a significant impact on future research in this field.

2.5 New Schlieren techniques

The last years have seen the development of new Schlieren techniques that utilise the concepts of other flow visualisation techniques. Particle Image Velocimetry (PIV) has had a particularly strong impact on these developments. It should be noted that it has been tried for some time to implement actual PIV techniques into the diagnostic tool set for high-speed compressible flows, but except for a few successful applications⁽²⁴⁾ these techniques have not yet been established for the investigation of hypersonic flows. The concept of PIV, however, has been used extensively in the development of a new Schlieren method known as 'Background-Oriented Schlieren'⁽²⁵⁾ or 'Synthetic Schlieren'⁽²⁶⁾. Distortions of a background pattern as a result of the light beam modifications discussed earlier are used to determine density gradients. Rangunath *et al*⁽²⁷⁾ introduced this technique to visualise hypersonic flows. At the current stage of the development, these techniques are still inferior to the classical Schlieren methods, both with respect to spatial and temporal resolution. While

Rangunath *et al*⁽²⁷⁾ demonstrated that these techniques can be used in hypersonic ground facilities, the results indicate that the aforementioned challenges apply equally well to these newer methods, that is, spatial resolution and luminosity in the test section still pose significant problems.

3.0 INTERFEROMETRY

3.1 Overview

Like Schlieren and shadowgraph techniques, interferometry has long been used as a flow-field diagnostic technique, particularly since lasers have become readily available. Many varieties of interferometry have been used to facilitate flow visualisation and/or quantitative analysis including differential, Michelson, and Mach-Zehnder. More recently, the preferred method for impulse facilities has been holographic interferometry which is less demanding on the quality of the optical components and on the stability of the system.

From a quantitative point of view, interferometry is best suited to density measurements in two-dimensional flows. The theory and constants involved in the analysis of an interferogram are generally well understood and hence it is relatively easy to extract highly accurate measurements. However, interferometry is a line-of-sight technique and more complex flows are difficult to analyse without resorting to tomographic methods. Recent extensions of the technique have also allowed interferometry to be used for measuring ionisation levels, species concentrations and temperatures.

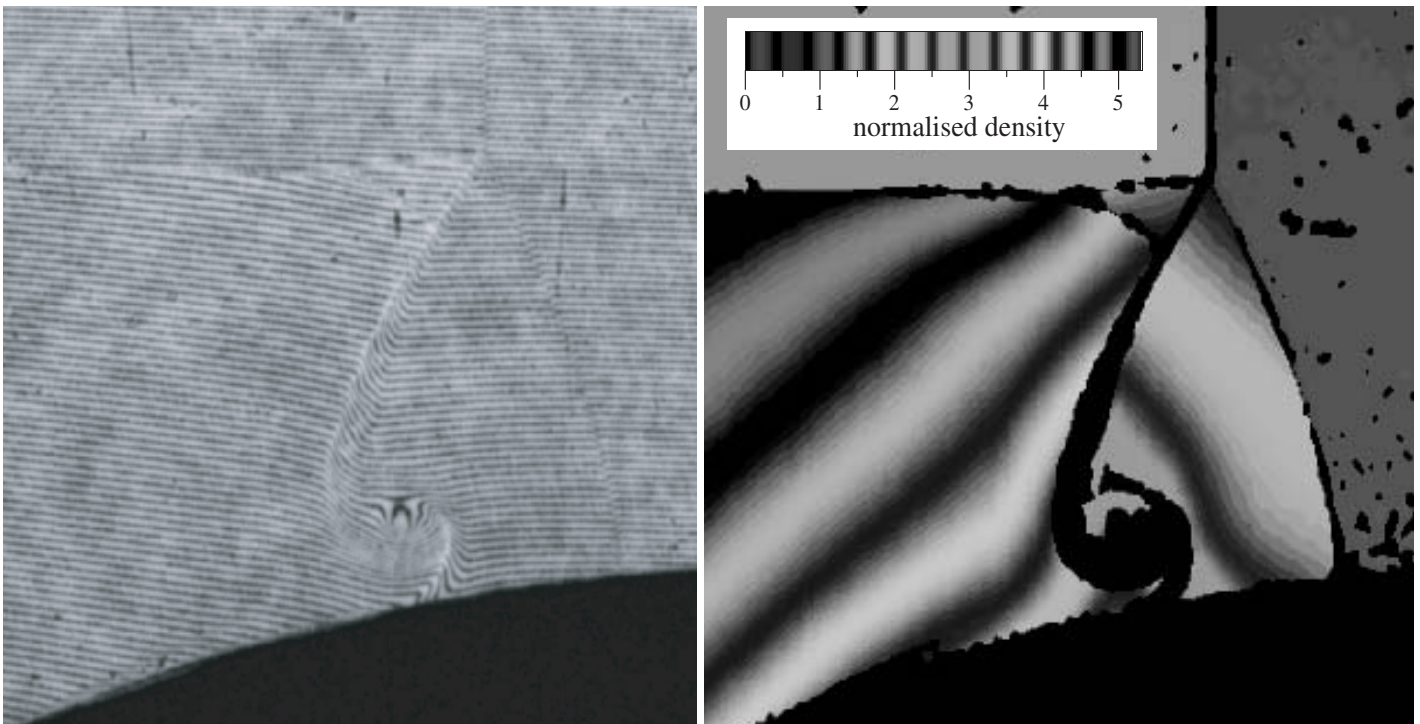


Figure 6. Holographic interferogram and processed density measurement for unsteady flow over a semi-circular cylinder (from⁽³⁴⁾). Flow is from left to right.

3.2 Fundamentals

An interferometer has two arms through which light is allowed to propagate. One of the arms contains the flow-field of interest while the other constitutes the reference arm which is used for comparison. A schematic layout of a Mach-Zehnder interferometer is shown in Fig. 5(a). In this arrangement a single pulse of light is divided into two arms in space by a beam splitter. The beams are later recombined by a second beam splitter allowing interference to occur. Holographic interferometers differ in that they have two arms in time rather than space – see Fig. 5(b). A reference beam is recorded on a holographic plate for a no-flow situation. This is achieved using a recording arm (different from the reference arm of a Mach-Zehnder interferometer) to make a holographic recording. During operation of the flow facility, a second, with-flow, hologram is recorded. The two holograms are later simultaneously reconstructed allowing for interference to be observed.

In either format, the light which passed through the test gas interacts with the flow resulting in a change in the speed of propagation and hence a change of the phase of the light. Depending on the magnitude of this phase shift, the test and reference beams can recombine constructively (in phase), destructively (180° out of phase), or anywhere in between. The phase shift, $\Delta\phi$, accumulated as the beam passes across a section of length l is given by

$$\Delta\phi = 2\pi (n - 1) l / \lambda \quad \dots (1)$$

where n is the refractive index of the gas and λ is the wavelength of the light. The refractivity of the atoms, molecules and ions in the gas is given by the Gladstone-Dale relation

$$n - 1 = \sum(G_i \rho_i) \quad \dots (2)$$

where G_i is the Gladstone-Dale coefficient for species i , and ρ_i is the species density. G is weakly dependent on the illumination wavelength but is otherwise constant. G for a non-reacting air mixture is generally taken as $2.3 \times 10^{-4} \text{m}^3/\text{kg}$. For a single species (or non-reacting) flow, Equations (1) and (2) can be combined to give the flow density as

$$\rho = \rho_0 + (p - p_0) \lambda / (G l) \quad \dots (3)$$

where p is the fringe shift ($= \phi/2\pi$) and subscript 0 refers to a reference point in the interferogram where the density is presumed to be known (usually the free-stream).

The fringe shift (or phase shift) must be extracted from the interferogram to obtain the density. This is usually achieved by a combination of a fast-Fourier transform algorithm coupled with a phase unwrapping routine⁽²⁸⁻³¹⁾. These methods are generally thought to be able to resolve phase changes down to one tenth of a fringe shift. For further details on holographic interferometry, readers are referred to the book by Vest⁽³²⁾.

3.3 Application of standard interferometry

Interferometry systems have become standard for use on a number of impulse facilities – mostly dominated by holographic systems. They typically consist of a pulsed laser (Nd:YAG or ruby) timed to produce light during the test time of the facility. The reference image is holographically recorded immediately prior to firing the facility while the test image is taken during the steady flow time. After processing, the holographic plate is used to reconstruct the beams forming the interferogram. Natural flow luminosity is less of a problem than for other techniques as it is easily filtered either spatially or spectrally.

Many groups have publications displaying interferometric results and it is only possible to cover a few examples here. A wide variety of images have been produced at the Tohoku University, in Sendai, Japan⁽³³⁾. An example of recent work is shown in Fig. 6⁽³⁴⁾. A non-stationary shock wave is viewed propagating over a semi-circular cylinder. In the interferogram, finely spaced fringes are observed and these are processed to provide the density distribution throughout the flow. The technique allows clear visualisation of multiple shocks as well as the shear layer and associated vortices. A similar type of system was developed and used on the T5 shock tunnel to image complex shock-shock interactions in hypersonic flow⁽³⁵⁾. Holographic interferometry has also been performed on a model in a ballistic range^(36,37).

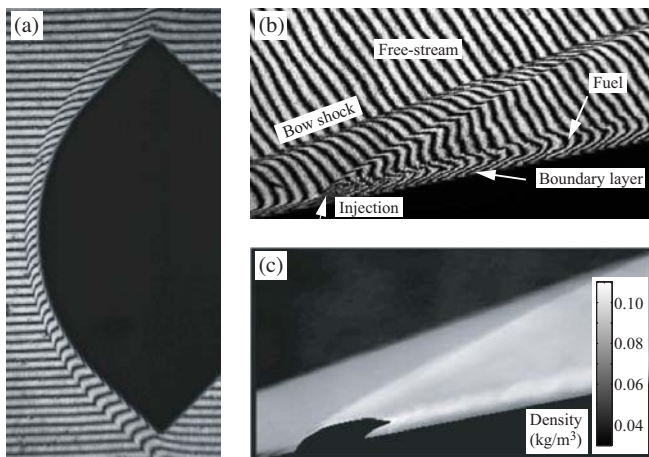


Figure 7. Selected interferometry images of hypersonic flow. (a) Interferogram of flow over a re-entry capsule travelling at 10 km s^{-1} ; (b) Interferogram of flow on the intake of a supersonic combustion ramjet with fuel injection (from⁽³⁸⁾); (c) Density distribution obtained from processing the image of the interferogram in (b).

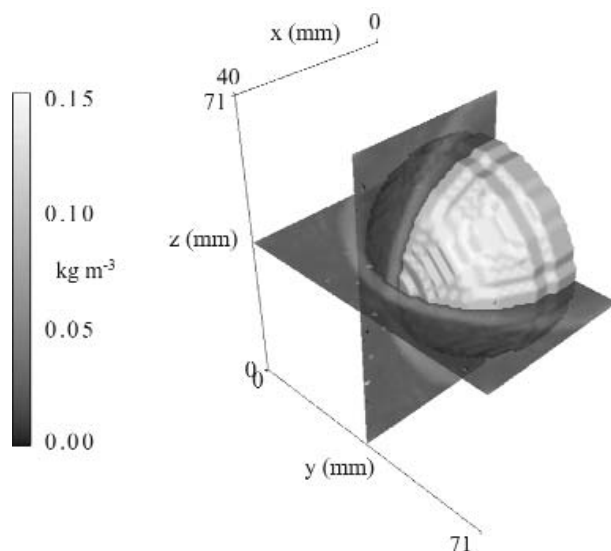


Figure 8. Tomographic reconstruction of flow over a hemisphere⁽⁴⁴⁾.

Holographic interferometry systems have been developed for quantitative imaging at the Centre for Hypersonics, in the University of Queensland, Australia. These systems are all based around double pulse holographic interferometry using a Nd:YAG laser recording on holographic plates. The systems have been used to image flows with speeds up to 10 km s^{-1} and to examine combusting flows relevant to supersonic combustion ramjets (scramjets). Figure 7(a) shows an interferogram for flow over a re-entry capsule in the X2 super-orbital expansion tube. Flow is from left to right and the test gas is air travelling at 10 km s^{-1} . Flow on the inlet of a model scramjet was imaged in the T4 shock tunnel. An interferogram is shown in Fig. 7(b). The image clearly allows the identification of the shock waves emanating from the front of the body and from the fuel injection, as well as the location of the boundary layer and the fuel⁽³⁸⁾. The image was processed to obtain the flow density as shown in Fig. 7(c) (the fringes could not be resolved just above the injection point and hence the analysis cannot be completed there). The obtained values are valid except in

regions where the fuel is present (the lighter coloured region just above the model surface). In this region, the phase shifts due to the test gas and the fuel cannot be separated without resorting to other assumptions⁽³⁹⁾.

3.4 Recent advances

Interferometry has evolved in a range of ways allowing the more accurate measurement of flow conditions, the study of a wider range of flows, and to measure other parameters apart from density. A major challenge in processing interferograms is the removal of noise through Fourier processing, without losing critical flow information. An alternative approach to Fourier filtering is the phase shifting or two-reference arm holographic interferometry method. In this arrangement, the no-flow and with-flow holograms are recorded with separate reference beams. In the construction process, the relative phase of the two reconstruction beams can be varied so that interferograms are recorded with varying phase differences. This allows the removal of noise and the purported increase in sensitivity is up to one twentieth of a fringe, a factor of two improvement. Such a system has been developed for the high enthalpy facility in Göttingen, Germany (HEG) and has been used to study a variety of flows⁽⁴⁰⁾.

The path length of the gas that the light passes through in the test section limits the sensitivity of interferometry systems. The length is generally a fixed parameter and hence there is an inherent lower limit to density variations that can be detected. An approach to increase the sensitivity of the system is to implement a multi-pass system. A pair of mirrors is used to pass the light multiple times through the test section before recording on the holographic plate. This has been successfully implemented in hypersonic flow in the F4 wind tunnel⁽⁴¹⁾.

Interferometry is, by nature, a line of sight technique so that it is ideally suited to two-dimensional flows. A number of methods have been developed to apply interferometry to more complicated model configurations. For axisymmetric models, it is possible to obtain quantitative information via a process called Abel Inversion. This mathematical analysis extracts the density as a function of radius from a single interferogram. Flows over spheres and cones have been studied in hypersonic flows clearly demonstrating the applicability of the technique⁽⁴²⁾. For more complicated flows, it is necessary to resort to multiple imaging from various angles – the more images recorded, the more accurate the technique. A single shot application of the technique requires large resources so the approach is generally to record single images over multiple shots and rely on conditions being repeatable. Studies of shock tunnel flows have been used to demonstrate the technique and to investigate the requirements to provide good quality images^(43,44). An example for the flow over a hemisphere is shown in Fig. 8⁽⁴⁴⁾.

In general, interferometry is performed with any available light source with little consideration required for selecting the wavelength. Spectrally selective methods however can lead to the measurement of quantities not normally associated with interferometry. In high temperature flows, the presence of electrons leads to a contribution to the refractivity of the gas which is different from the heavy particles. The refractivity takes the form⁽⁴⁵⁾

$$n - 1 = KN_e \lambda^2 \quad \dots (4)$$

where N_e is the electron number density and K is a collection of fundamental constants. The key difference from Equation (2) is the wavelength dependency which leads to fringe shifts being dominated by electron contributions at long wavelengths, and by heavy particles at short wavelengths. By utilising a recording system with two separate wavelengths, it is possible to determine both the heavy particle density as well as the electron concentration⁽⁴⁶⁾. An example of such a measurement is shown in Fig. 9⁽⁴⁷⁾, here an air test gas was studied at a free-stream velocity of 10.7 km s^{-1} leading to approxi-

mately 5% ionisation behind the bow shock on a horizontal cylinder. Later comparisons with numerical simulations showed excellent agreement⁽⁴⁸⁾. It was also noted that a measurement of both the flow density and the electron concentration can be combined via the Saha equation to yield the flow temperature in regions of chemical equilibrium⁽⁴⁹⁾.

More careful selection of laser wavelength can lead to the measurement of species concentration, or as a technique to enhance the sensitivity of normal interferometry. The method, termed near-resonance holographic interferometry, relies on the variation of the refractive index near the transition line of a species⁽⁵⁰⁾

$$n_{\lambda} - 1 = \frac{e^2 N f \lambda_0}{16 \pi^2 \epsilon_0 m_e c^2 \left(\frac{1}{\lambda_0} - \frac{1}{\lambda} \right)} \quad \dots (5)$$

where N is the species number density, f is the oscillator strength, and other symbols take their previously defined values. With laser detunings of the order of hundreds of picometres, an increase in sensitivity of one or two orders of magnitude has been achieved, and studies have been completed of blunt body flows⁽⁵¹⁾, boundary layer flows⁽⁵²⁾ and for investigating the design of a toroidal ballute⁽⁵³⁾. The level of enhancement possible is illustrated in Fig. 10 where non-resonant and near-resonant images of flow over a vertical cylinder are shown side by side⁽⁵⁴⁾. While the location of the bow shock is clearly evident in the near-resonant case, only very small fringe shifts are discernible when standard (non-resonant) interferometry is applied.

3.5 Future directions

Interferometry is in general a mature technology with developments mostly likely to result from technological improvements. The standard double pulse application method of holographic interferometry is a single shot method requiring the development of a holographic plate before the image can be observed. An alternative approach is to record a reference hologram, develop the plate, and then replace it back in the optical system. This allows real time recording of images directly to a video camera⁽⁵⁵⁾. For impulse facilities, this approach coupled with high-speed video cameras opens the possibility for multiple images in a single shot. Alternative holographic materials are also becoming available⁽⁵⁶⁾ allowing development in situ which avoids the difficult process of carefully placing the developed plate back in the experimental arrangement. An alternative approach is to by-pass the plate process altogether and record the holograms digitally⁽⁵⁷⁾. This has been limited in the past by the resolution of CCD cameras but these are now developing towards the stage where they will have sufficient resolution to provide good quality images.

Holography is a three-dimensional recording method for which only two dimensions are used in the holographic interferometry arrangement shown in Fig. 5. This occurs as the flow is illuminated by a plane wave effectively removing the third dimension (parallel to the laser propagation direction). To achieve three-dimensional recording, the flow must be illuminated by a diffuse laser source that passes through the flow and is recorded on a holographic plate. Because of the diffuse laser beam, the holographic plate has to be placed in close vicinity to the model in order to provide sufficient exposure. In most hypersonic impulse facilities, this poses a technological challenge as the flow is generally established in the centre of a usually large test section. Furthermore, this technique would be more susceptible to detrimental influences by luminosity in the test section as the holographic plate is typically placed next to the test section with no other optical components in between. Finally, in order to provide a reasonably wide range of viewing angles, the system requires illumination from a large area relative to the model size and needs to be recorded on a similarly large plate. Technological developments may lead to this becoming realisable in

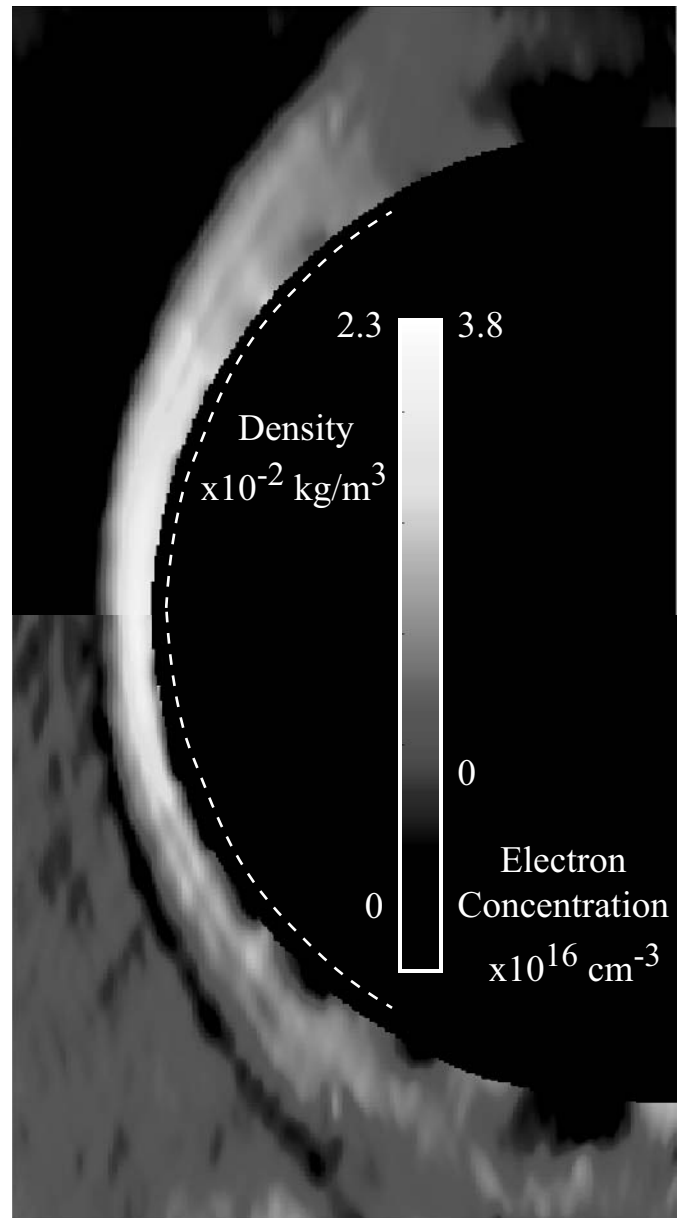


Figure 9. Measured quantities from two-wavelength holographic interferometry. The upper half shows the density distribution; the lower half shows the electron number density. The dotted line shows the position of the model. The dark region in the flow immediately adjacent to the model could not be processed due to poor fringe visibility⁽⁴⁷⁾.

the near future for hypersonic test facilities, but so far applications have been limited to shock tube flows where test section access and luminosity do not present a problem^(3,5,32). It ought to be mentioned that such a recording does not generate a three-dimensional image of the flow but a large number of two-dimensional projections^(5,58).

4.0 FLUORESCENT IMAGING

4.1 Overview

The theory of laser-induced fluorescence (LIF) is well developed and details can be found in various places in the literature⁽⁵⁹⁻⁶¹⁾. It can be described most simply as the absorption of laser light by an optically allowed transition in an atom or molecule, followed by the

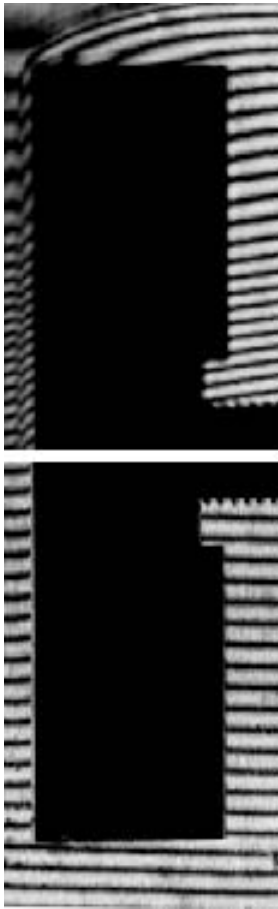


Figure 10. Comparison between a near-resonant interferogram (upper half) of flow over a cylinder with a non-resonant interferogram of the same flow (lower half).

subsequent isotropic emission of radiation (fluorescence). However, this two-step description does not lend itself to a true appreciation of the complexities of the process, which become apparent when one considers aspects such as saturation, inhomogeneous broadening, and energy-transfer mechanisms. The traditional approach to introducing these concepts is to begin with a two-level model of the absorber, which may be either an atom or a molecule, and gradually increase the degree of sophistication by adding more processes (e.g., energy transfer, quenching), which generally translates into adding more levels to the model. Nevertheless, the two-level model⁽⁵⁹⁾ encompasses the majority of the important features of laser-induced fluorescence for the situation in which it usually applied, i.e., the weak-excitation (low laser irradiance) limit.

Although originally applied only as a point-wise technique, LIF has been extended to an imaging method called planar laser induced fluorescence (PLIF)⁽⁶¹⁻⁶³⁾ by utilising a sheet of laser light and a two-dimensional detection system (typically collection optics in conjunction with intensified charge-coupled devices, or ICCDs). The basic principles remain the same though. A laser light source is tuned to a resonance transition in an absorber and a certain fraction of the absorbing state population is transferred to an excited state. The absorber then spontaneously radiates after some lifetime characteristic of the excited state, returning either to the original or to some intermediate level. This radiation, or fluorescence, is generally isotropic, although in some cases it can show a certain degree of anisotropy⁽⁶⁴⁾. The excited absorber will often be de-excited by other competing mechanisms, both radiative and non-radiative. For example, if the excited absorber undergoes a collision, then a non-radiative transition may occur, known as collisional quenching. Other competing processes, such as rotational energy transfer (RET)^(65,66) and vibrational energy transfer (VET)^(60,67) need to be considered, but generally speaking, collision-induced transitions add a temperature- and species-dependent factor to the fluorescence signal which complicates interpretation and decreases the magnitude of the signal. RET and VET are generally treated in the same way as collisional quenching, with rate equations, using experimentally-determined rate coefficients, to describe their contribution to the loss from the upper laser coupled state⁽⁶⁸⁾.

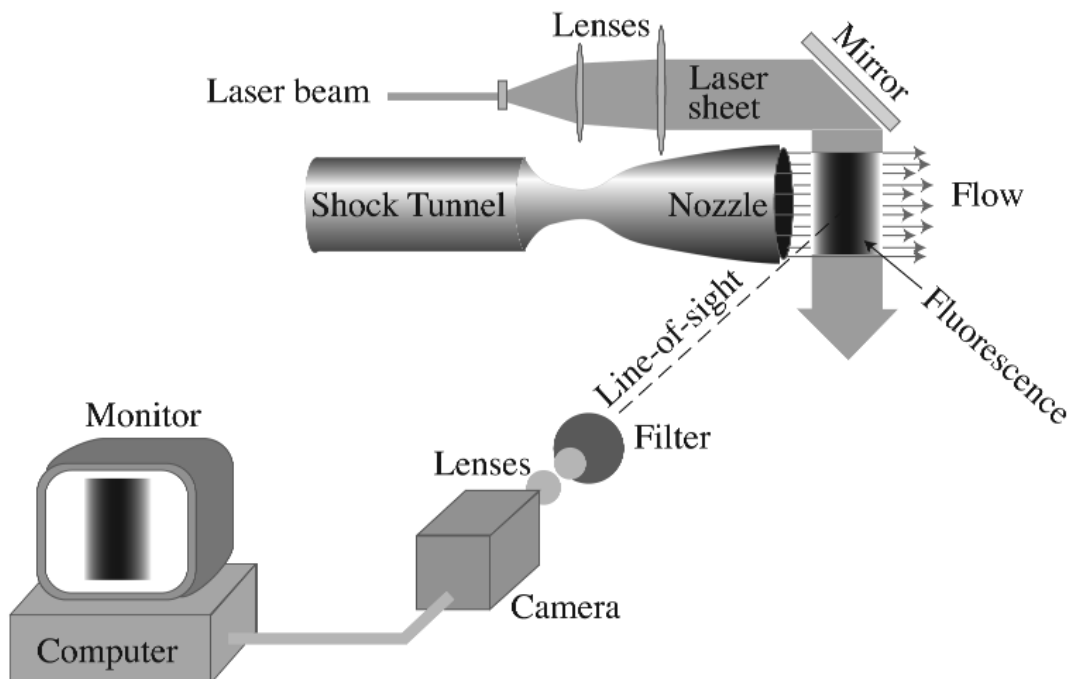


Figure 11. Schematic diagram of the experimental arrangement for planar laser induced fluorescence measurements.

Much of the theoretical development for LIF involves producing a closed-form solution to the equation describing the fluorescence signal, and developing strategies to isolate the signal dependencies on specific physical parameters, such as temperature, concentration or velocity. There are two alternative approaches to the theoretical description of the LIF process. The first is the quantum-mechanical formulation, which involves solving the density matrix for the two-level absorber⁽⁶⁹⁻⁷¹⁾. Collisional processes and spontaneous emission are included in terms of phenomenological decay constants. The alternative approach is to use a semi-classical rate equation analysis⁽⁷²⁾. The latter procedure is easier to conceptualise and solve mathematically, but has a limited range of validity and may omit possible coherence effects⁽⁷³⁾. The theory presented in this review is based on the semi-classical approach. Palma *et al*⁽⁶⁰⁾ provide a discussion of the validity of the rate-equation analysis upon which this semi-classical approach is based.

The fluorescence-signal equation simplifies in the limits of high and low laser irradiances. In the low-irradiance limit, the fluorescence signal varies linearly with laser irradiance and allows easy interpretation of experimental results. In the high irradiance limit, the absorption transition becomes saturated and the fluorescence is characterised by its reduced dependence on irradiance and collisional quenching^(72,74). However, accurate saturated LIF measurements are difficult to achieve in practice due to the inability to ensure complete saturation across the entire spatial and temporal profiles of the laser pulse. In this review, we restrict ourselves to the two-level model using the low radiance approximation.

Figure 11 is a simplified illustration of a PLIF setup. The format for the setup is generally as follows. Light from a narrowband pulsed laser (often pumped by a Nd:YAG or an excimer laser) is formed into a sheet and used to probe a particular species in the flow (often either nitric oxide, NO, or the hydroxyl radical, OH), exciting the target species to an energy level, from which it subsequently fluoresces. An intensified camera collects the fluorescence signal at right angles to the sheet, obtaining, in the case of pulsed flows, one image per flow pulse, i.e. shock tunnel or shock tube run. Provided the assumptions of linear fluorescence, weak excitation, negligible laser beam attenuation, and negligible radiation trapping are valid, the fluorescence signal level is given by⁽⁷⁵⁾

$$S = \frac{E_p}{A_{las}} \frac{\chi_a P}{kT} \left(\sum_i f_b B g \right) \left(\frac{A}{A+Q} \right) C_{opt} \dots (6)$$

Here the summation is over all transitions induced by the laser; E_p is the laser energy per pulse; A_{las} is the cross-sectional area of the laser sheet; χ_a is the mole-fraction of the absorbing species; P is the pressure; k is the Boltzmann constant; T is the temperature; f_b is the Boltzmann fraction of the absorbing state; B is the Einstein coefficient for absorption; g is the spectral overlap integral; A is the effective rate of spontaneous emission for all directly and indirectly populated states; Q is the total collisional quenching rate of the electronic excited state; and C_{opt} is the efficiency with which photons emitted from the gas are collected by the optical system and converted to photoelectrons in the ICCD camera. C_{opt} depends on the arrangement of the collection optics, spectral filtering, temporal gating, photocathode quantum efficiency, and intensifier gain. The term $A/(A+Q)$ is known as the fluorescence yield, Φ .

Through an understanding of the theoretical basis of PLIF, different researchers have been able to apply the method to flow imaging, thermometry (rotational and vibrational temperature measurements), velocimetry, flow-tagging, pressure measurements, and mixing studies. The following sections describe sample applications to impulse facilities.

4.2 Flow imaging

One of the biggest advantages of PLIF over other common flow visualisation techniques is its ability to image complex flows. In PLIF, only the volume illuminated by the laser sheet is probed,

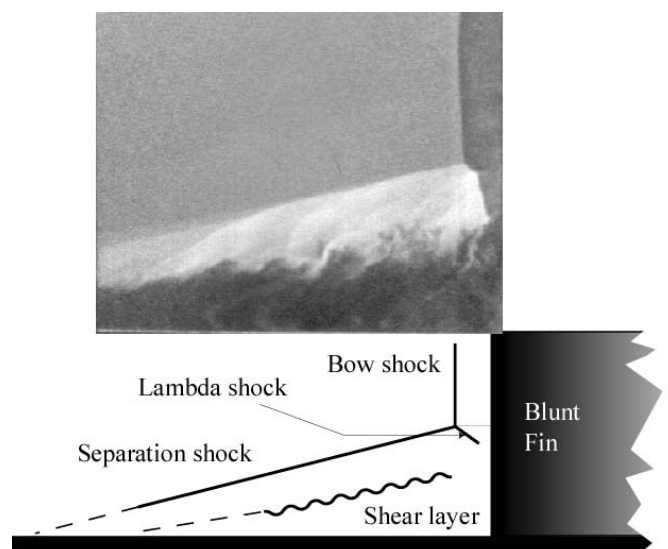


Figure 12. PLIF image and schematic of separated flow upstream of a blunt fin in a hypersonic flow⁽⁷⁶⁾.

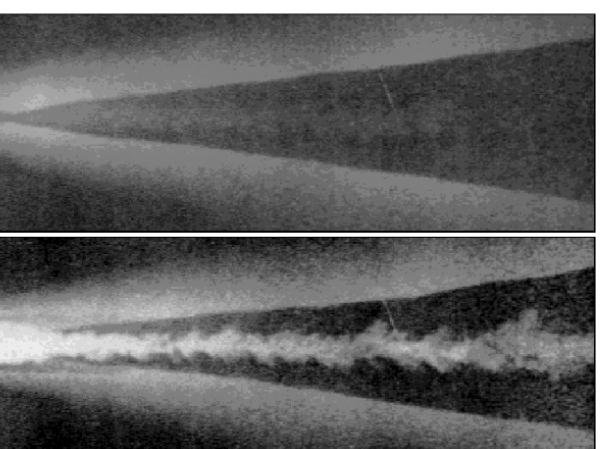
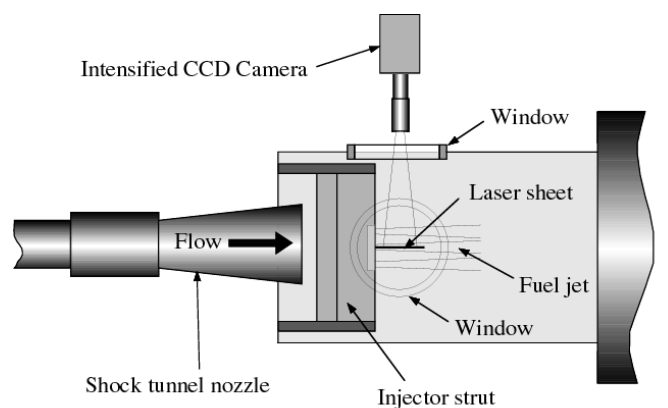


Figure 13. Schematic diagram and images of PLIF studies of hypersonic mixing⁽⁸²⁾. (a) Flow without injection; (b) Flow with fuel injection.

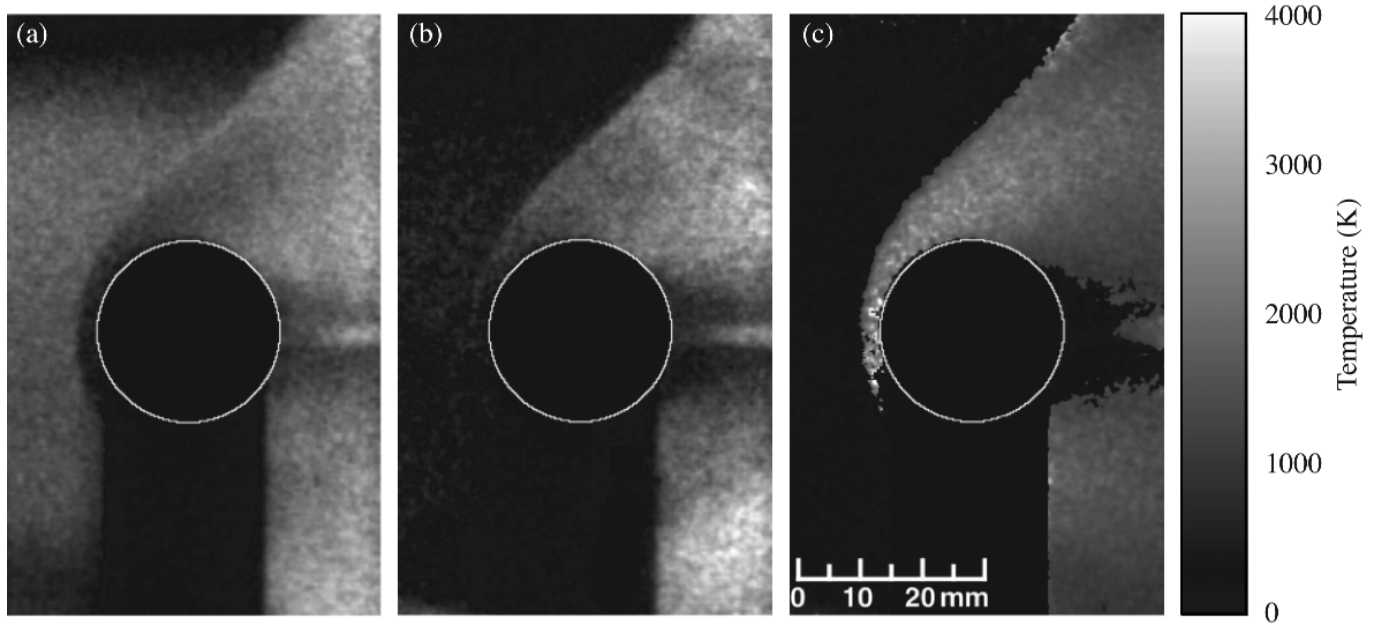


Figure 14. PLIF temperature imaging of a 4-1MJ/kg flow over a cylinder⁽⁶⁸⁾.
 (a), (b) Raw PLIF images;
 (c) Rotational temperature distribution obtained from combining the images shown in (a) and (b).

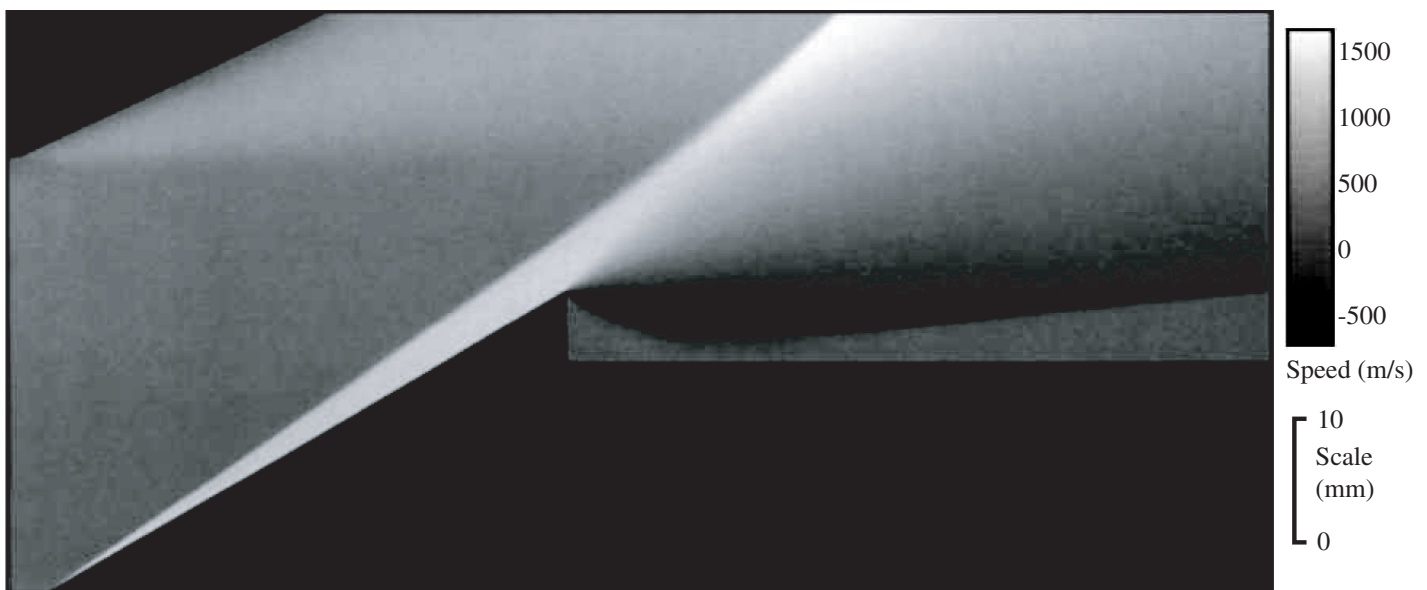


Figure 15. PLIF velocity measurement of Mach 7 flow around a 30° half-angle cone⁽⁹⁶⁾.

reducing measurements to effectively a two-dimensional cross-section of the flow. This is in contrast to the previously discussed techniques which result in images that have contributions integrated along the path of the illuminating light.

A prime example of this advantage is illustrated in the experiments of Fox *et al.*⁽⁷⁶⁾ who used fluorescence imaging to investigate the separated flow upstream of a blunt fin in a hypersonic free-stream with a transitional boundary layer in the free-piston shock tunnel T3. A PLIF image, such as that shown in Fig. 12, allows the clear identification of the flow structures. Studies were made to identify the flow development during the test time of the tunnel and these showed that the test time in T3 was long enough to achieve a steady flow over the blunt fin. Transient shock phenomena have also been investigated⁽⁷⁷⁾ while the development of separated flow in the near wake of a cone and a wedge has been visualised in the hypersonic free-stream of the T2 free-piston driven shock tunnel⁽⁷⁸⁾.

A major field of study in impulse facilities over recent years has been the development of supersonic combustion ramjets (or scramjets). Here mixing studies are of prime importance as fuel, injected into a hypersonic flow, must react with the incoming oxygen for combustion to result in the generation of thrust. Optical techniques provide an ideal tool for investigating these types of flows by either detecting NO naturally present in the free-stream of these facilities, or adding it into the injected fuel stream. Early work of this type was conducted in lower speed facilities^(79,80). More recently, many examples of this type of imaging have become available. For example, a variety of fuel injection schemes have been studied in the T3 shock tunnel⁽⁸¹⁾. The experimental arrangement for these measurements and sample images are shown in Fig. 13. Here fuel is injected into the flow using a strut and the region immediately downstream of injection was observed. In an attempt to quantify the relative fuel concentrations, a detection scheme was developed for

which the fluorescent signal was proportional to the NO concentration. The amount of fuel was clearly visualised after which the images were compared with numerical simulations⁽⁸²⁾ and further studies using an injection mixture of He/NO were also completed⁽⁸³⁾. There has been continuing work focussing on imaging the mixing fraction to better understand the processes involved⁽⁸⁴⁾. Evidence of combustion has also been examined through visualising the presence of the OH molecule^(85,86).

4.3 Thermometry

The major quantitative measurement that can be made is the determination of the flow temperature. This is commonly achieved by obtaining PLIF images using two separate excitation lines. These images provide relative measurements of the populations of the energy levels of the lower states of the transitions. Under the assumption of thermal equilibrium, these populations are linked by the Boltzmann distribution which can be applied to give the flow temperature. Where the two levels have the same vibrational quantum number but different rotational quantum numbers, the temperature is the rotational temperature which, in these type of flows, is presumed equal to the translational temperature. It is also possible to measure the vibrational temperature by an appropriate choice of transitions.

In circumstances where equipment limitations preclude the simultaneous probing of different lower laser-coupled states, signals from probing such states must be accomplished with a single-laser, single-camera arrangement during separate shots on the shock tube or shock tunnel facility. Such an approach relies on high shot-to-shot repeatability of the facility, careful monitoring of the laser sheet energy distribution for each shock tube/tunnel shot and the acquisition of sufficient data to perform statistically-significant shot averaging.

The first applications of two-line and multi-line PLIF thermometry to a shock tube flow used two independent laser/camera systems that image the same flow area, usually with some small time separation (of order of hundreds of nanoseconds)^(87,89). The lasers and cameras are synchronised with the facility to provide images at an appropriate time during the steady flow. To improve on noise, multiple images can be recorded in successive shots and averaged. Thermometry has since been extensively implemented on a range of other facilities. These include the AEDC impulse facility⁽⁹⁰⁾, the HEG shock tunnel⁽⁹¹⁾, and the HYPULSE expansion tube⁽⁹²⁾.

One of the first applications of fluorescence thermometry to a free-piston shock tunnel flow⁽⁹³⁾ used the laser-induced pre-dissociation fluorescence (LIPF) to avoid the effects of collisional quenching and to measure vibrational temperature in a bow shock layer. Pre-dissociation fluorescence does not have a strong quenching dependence because the pre-dissociation rate of the laser-populated level is much faster than the collisional quenching rate. As a consequence, the fluorescence yield is essentially quenching independent. Under such conditions, the vibrational temperature of molecular oxygen was measured in the shock layer around a circular cylinder in a pulsed hypersonic free-stream, at a moderate stagnation enthalpy. The measurements were produced by the excitation of oxygen molecules in the flow with the tuned, narrowband output of an ArF excimer laser. The close coincidence of two transitions from two different lower vibrational states allowed the determination of the relative population of these states and thus the vibrational temperature of the oxygen molecules. However, the extremely low fluorescent yield of the LIPF technique resulted in high experimental uncertainties and was a major limitation in comparing the experimental results with CFD simulations.

In a separate investigation using a single laser/camera system in the free-piston shock tunnel, a Raman-shifted tunable excimer laser was used to excite nitric oxide molecules in the flow⁽⁶⁸⁾. Two different flow-fields were examined to test the difficulties associated with applying the technique to shock tunnels: the blunt

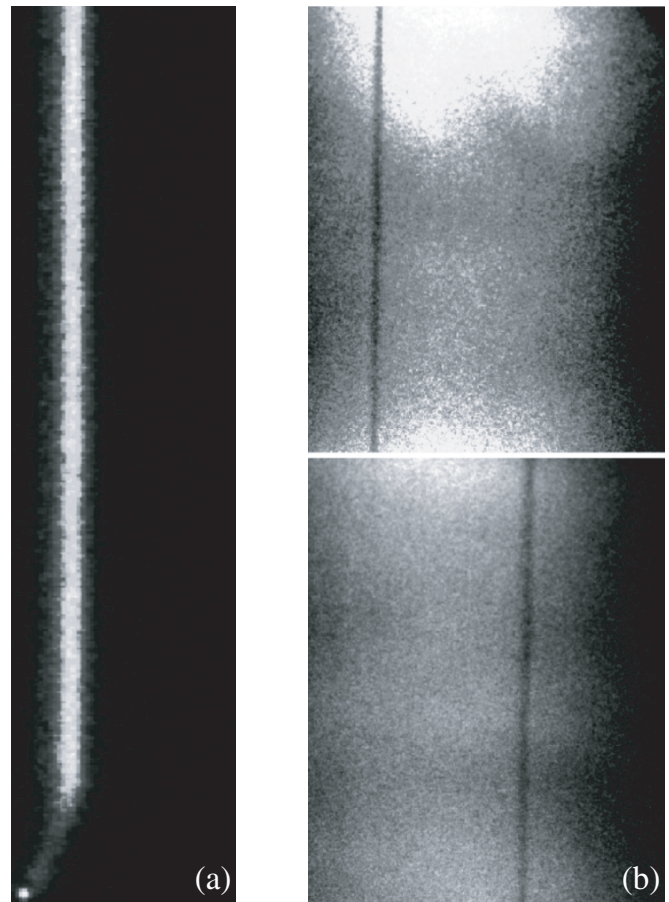


Figure 16. Flow tagging velocity measurements. (a) Single shot image of tagged NO molecule⁽¹⁰⁰⁾; (b) Laser enhanced ionisation velocimetry images at two separate tag-probe delays⁽¹⁰¹⁾.

body flow produced by a 25mm diameter cylinder and the oblique shock and expansion fan produced by a 35° half-angle wedge. For the cylinder, the maximum flow enthalpy was limited to 4 MJ/kg due to high flow luminosity which is produced by metallic contaminants in the flow. A reflective filter was used to reduce the influence of flow luminosity making these measurements feasible. A selection of images and a temperature measurement are shown in Fig. 14. The PLIF arrangement permits mounting of the model from the side of the test section rather than from behind and hence it is possible to obtain measurements in the wake flow as well as in front of the body. Free-stream temperature measurements were reported as being in excellent agreement with those predicted from numerical flow calculations. Larger uncertainties were observed for the high-temperature post-shock results. Several higher enthalpy shots (14MJ/kg) were also performed with the wedge and showed an insignificant amount of contaminant emission⁽⁹⁴⁾.

4.4 Velocimetry

The approach to velocimetry using PLIF is two-fold relying on Doppler methods or on flow tagging. In the Doppler approach, excitation occurs at an angle to the flow so that the illuminating radiation is Doppler shifted on to, or away from an optical transition depending on the speed of the flow along the direction of the laser beam. By careful selection of transition and tuning, the intensity of the resulting fluorescence can be related to the velocity of the flow⁽⁹⁵⁾. Planar laser-induced fluorescence of nitric oxide was used to measure a component of the velocity field for the Mach 7 flow around a 30° half-angle, 50mm diameter cone mounted to a long, 38mm diameter

shaft, or 'sting'⁽⁹⁶⁾. An image is shown in Fig. 15. Transverse velocities were measured in the free-stream, the shock layer, and the separated region at the junction between the cone and the sting. For most of the flow-field, the uncertainty of the measurements was between ± 50 and $\pm 100\text{ms}^{-1}$ for velocities ranging from -300 to $1,300\text{ms}^{-1}$, corresponding to a minimum uncertainty of $\pm 5\%$. The measurements were compared with results generated by the commercial computational fluid dynamics (CFD) code CFD-FASTRANTM. The agreement between the theoretical model and the experiment was reported as being reasonably good, with CFD accurately predicting the size and shape of the shock layer and separated region behind the cone as well as the magnitude of the gas velocity near the reattachment shock. However, the magnitude of the velocity in the shock layer and gas expansion was reported as differing somewhat from that predicted by CFD. The discrepancies were attributed to a small systematic error associated with laser-beam attenuation and also to inexact modelling of the flow-field by CFD⁽⁹⁶⁾.

Raman excitation plus laser-induced electronic fluorescence (RELIEF) can be used to image the motion of oxygen molecules in air and other gas mixtures⁽⁹⁷⁾. This is accomplished by tagging oxygen molecules through vibrational excitation and imaging them after a short period of time by laser-induced electronic fluorescence. The vibrational lifetime of oxygen is sufficiently long and the signal sufficiently strong to allow this technique to be used over a wide range of flow conditions from low subsonic to hypersonic and in a variety of gas mixtures including high humidity environments. The use of a molecular tagging technique such as this is critical for environments in which seeding is impossible or unreliable and for measurements in which a wide range of scales needs to be observed simultaneously. Two experiments which have been conducted in medium- to large-scale facilities have been reported⁽⁹⁸⁾. At the Arnold Engineering Development Center, RELIEF was used to examine velocity in a 1m diameter tunnel for applications in the area of engine testing. At the NASA Langley Research Center, RELIEF has been used to examine supersonic mixing of helium in air in a coaxial jet in association with studies of fuel-air mixing in hypersonic engines. The RELIEF method has yet to be applied to pulsed hypersonic flows.

A new variation of molecular flow tagging velocimetry for hypersonic flows has been developed based on laser-induced fluorescence⁽⁹⁹⁾. A thin line of nitric oxide molecules was excited with a laser beam and then, after a time delay, a fluorescence image of the displaced line was acquired. One component of velocity was determined from the time of flight. This method was applied to measure the velocity profile in a Mach 8.5 laminar, hypersonic boundary layer⁽¹⁰⁰⁾ in the T2 free-piston shock tunnel of the Australian National University (ANU). A sample image is shown in Fig. 16(a) in which the tagged line propagates with the flow moving from left to right. The line can be seen to be deformed in the boundary layer on a flat plate at the bottom of the image. The single-shot velocity measurement uncertainty in the free-stream was found to be 3.5%, based on 90% confidence. The method was also demonstrated in the separated flow region forward of a blunt fin attached to a flat plate in a Mach 7.4 flow produced by the T3 free-piston shock tunnel at ANU. The measurement uncertainty in the blunt fin experiment is approximately 30%, owing mainly to low fluorescence intensities, which according to the authors could be improved significantly in future experiments. This velocimetry method is applicable to very high-speed flows that have low collisional quenching of the fluorescing species. It is particularly convenient in facilities where planar laser-induced fluorescence is already being performed.

Another novel method⁽¹⁰¹⁾ for measuring the velocity by tagging in high-speed flows has been developed and tested using laser-enhanced ionisation (LEI)⁽¹⁰²⁾ to ionise sodium atoms and then detecting this neutral atom depleted region using PLIF. The atoms are ionised via a three-step process which includes excitation using two tunable dye-lasers followed by collisional ionisation. The exciting laser beams are tightly focussed and passed through the test

gas leaving a thin zone with better than 50% depletion of sodium atoms. At a short time later (of order 100-200ns), the flow is probed by a laser beam formed into a sheet tuned to the 589nm sodium atomic transition. The fluorescence is detected by a fast-gated intensified CCD camera yielding a two-dimensional image of the flow. The depleted line moves in this time reflecting the local velocity of the flow. This approach has been applied to measure velocities in a shock tube. Free-stream images are shown in Fig. 16(b) where the tagged line, moving left to right, is imaged at two different delays in successive shots. Free-stream values along with the velocity profile behind a cylinder were also measured in a super-orbital flow facility⁽¹⁰³⁾. Velocities in the free-stream at a super-orbital condition were measured yielding $9.20 \pm 0.3\text{km}^{-1}$. This result compared favourably with the flow speed determined from the measured shock speed in their facility.

4.5 Future directions

PLIF is a comparatively new visualisation technique with its complete benefits yet to be fully exploited. In its current format, there is a wide range of flows that could be better visualised by its implementation. Its restrictions lie mostly at higher velocities where background luminosity cannot be filtered enough to allow the signal to be observed. The main species of interest have been limited to NO and OH mainly due to their large transition probabilities, optically accessible transitions, relevance to hypersonic flows and strong non-resonant fluorescence. One can envisage the expansion of the technique to detect other types of species present in hypersonic flows. This will depend on the development of improved filtering techniques and on the availability of more sensitive cameras and/or higher energy lasers. The most widespread use of PLIF has been largely for qualitative imaging in hypersonic flow facilities, as quantitative versions of this technique are often single-purpose expert systems. However, the method's inherent potential for extending the amount of quantitative measurements is currently being further developed. As discussed, temperature and velocity are regularly measured but scope exists for the determination of other quantities such as species concentration and pressure.

5.0 CONCLUSIONS

The role of optical imaging techniques in past, present and future research in hypersonic impulse facilities has been discussed, and the challenges and advantages of these systems have been highlighted. It can be anticipated that the classical density-sensitive visualisation techniques will remain crucial diagnostic tools for hypersonic flow research due to their simplicity and low cost implementation. A range of newer laser-based diagnostic techniques has been discussed and some of these are becoming standard methods in the quantification of hypersonic flows. While it is difficult to predict the future direction of optical techniques, it is clear that newer technologies such as high-speed cameras are likely to impact on their development. High energy lasers and more sensitive cameras can be expected to lead to new techniques extending the current range of quantities that can be imaged and optically measured in hypersonic flows.

ACKNOWLEDGEMENTS

The authors would like to thank a wide variety of current and past postgraduate students, colleagues, and other research groups for their input and assistance in the preparation of this review. These contributions are too numerous to detail here but are generally acknowledged in references to appropriate publications in the text. The authors apologise if any relevant works have not been referenced in this review.

REFERENCES

1. STALKER, R.J. Modern developments in hypersonic wind tunnels, *Aeronaut. J.* 2006, **110**, (1103), pp 21-39.
2. BECK, W.H., SCHEER, M. and VETTER, M. An Examination of the Aachen Shock Tunnel TH2 Gas Flows Using the HEG PLIF Apparatus, Proc. 19th Int Symp Shock Waves, **1**, pp 321-326, Springer, 1995, Berlin, Heidelberg, 1995.
3. MERZKIRCH, W. *Flow Visualization*, 2nd ed., Ch 3, Academic Press, 1987, Orlando, USA.
4. SETTLES, G.S. *Schlieren and Shadowgraph Techniques*, Springer, 2001, Heidelberg, New York, USA.
5. KLEINE, H. *Flow Visualization*, in: *Handbook of Shock Waves*, **1**, Ch 5.1, pp 683-740, Academic Press, 2001, San Diego, USA.
6. CORDS, P.H. A High-resolution, high sensitivity color Schlieren method, *SPIE J.* 1968, **6**, pp 85-88.
7. OERTEL, H. and OERTEL, H. Jr Optische Strömungsmesstechnik, Braun, Karlsruhe, 1989. (in German).
8. KLEINE, H. Verbesserung optischer Methoden für die Gasdynamik, Thesis, Stosswellenlabor RWTH Aachen, Germany, 1994 (in German).
9. KLEINE, H., GRÖNIG, H. AND TAKAYAMA, K. Simultaneous shadow, Schlieren and interferometric visualization of compressible flows. *Optics and Lasers in Engineering*, 2006, **44**, (4), pp 170-189.
10. BIZE, D., DUNET, G., PHILBERT, M., ROBLIN, A. and SURGET, J. Schlieren device and spectroscopic measurements in F4, in: *Proc. of the NATO Advanced Research Workshop New Trends in Instrumentation for Hypersonic Research*, pp 135-151, Kluwer, Dordrecht, 1993.
11. VETTER, M. Hyperschallströmung von Modellen im Stosswellenkanal, Thesis, Stosswellenlabor RWTH Aachen, Germany, 1993 (in German).
12. KLEINE, H. and GRÖNIG, H. Colour Schlieren experiments in shock tube and tunnel flow, in: Proc Int Workshop on Strong Shock Waves, pp 41-48, Chiba University, 1992.
13. HONOUR, J. *Electro-Optical Camera Systems*, in: *High-Speed Photography and Photonics*, pp 134-149, Focal Press, Oxford, 1997 (reprinted by SPIE under the same title as SPIE PM120 in October 2002).
14. SMITH, G.W. *HIGH-SPEED CCD Camera Technology*, in: *High-Speed Photography and Photonics*, pp 81-98, Focal Press, Oxford, 1997 (reprinted by SPIE under the same title as SPIE PM120 in October 2002).
15. HASHIMOTO, T. and TAKAYAMA, K. Study of separated flows over double wedges and cones, in: Proc 24th Int Symp on Shock Waves, **1**, pp 479-485, Springer, Berlin, Germany, Heidelberg, 2005.
16. CRANZ, C. and SCHARDIN, H. Kinematographie auf ruhendem Film und mit extrem hoher Bildfrequenz, *Zeitsch. f. Physik*, 1929, **56**, pp 147-183.
17. PARKER, V. and ROBERTS, C. *Rotating Mirror and Drum Cameras*, in: *High-Speed Photography and Photonics*, pp 167-180, Focal Press, Oxford, 1997 (reprinted by SPIE under the same title as SPIE PM120 in October 2002).
18. HONOUR, J. A high resolution electronic imaging system for Schlieren recording, in: Proc 24th Int Congr high-speed Photography & Photonics, 2001, **4183**, pp 163-169, SPIE, Bellingham.
19. ETOH, T.G. TAKEHARA, K., OKINAKA, T., TAKANO, Y., RUCKELSHAUSEN, A. and POGGEMANN, D. Development of high-speed video cameras, in: Proc 24th Int Congr High-Speed Photography & Photonics, **4183**, pp 36-47, SPIE, Bellingham, 2001.
20. KLEINE, H., HIRAKI, K., MARUYAMA, H., HAYASHIDA, T., YONAI, J., KITAMURA, K., KONDO, Y. and ETOH, T.G. High-speed time-resolved color Schlieren visualization of shock wave phenomena. *Shock Waves* 2005, **14**, (5/6), pp 333-342.
21. WU, P.F.P. and MILES, R.B., Megahertz visualization of compression-corner shock structures, *AIAA J.* 2001, **39**, (8), pp 1542-1546.
22. ETOH, T.G., HATSUKI, Y., OKINAKA, T., OHTAKE, H., MARUYAMA, H., HAYASHIDA, T., YAMADA, M., KITAMURA, K., ARAI, T., TANIOKA, K., POGGEMANN, D., RUCKELSHAUSEN, A., VAN KULK, H., BOSIERS, J.T. and THEUWISSEN, A.J. An image sensor of 1,000,000 fps, 300,000 pixels and 144 consecutive frames. In: Proc 26th Int Congr. High-Speed Photography & Photonics, 2005, **5580**, pp 796-804, SPIE, Bellingham.
23. HIRAKI, K., KLEINE, H., MARUYAMA, H., HAYASHIDA, T., KITAMURA, K., YONAI, J., NAKAJIMA, T. and ETOH, T.G. Visualization of the unsteady flow field around spiked concave bodies in supersonic flow. In: Proc 12th Int Symp Flow Visualization, Göttingen, Germany.
24. HAERTIG, J., HAVERMANN, M., REY, C. and GEORGE, A. Particle Image Velocimetry in Mach 3-5 and 4-5 Shock Tunnel Flows. *AIAA J.* 2002, **40**, (6), pp 1056-1060.
25. MEIER, G.E.A. Computerized background-oriented schlieren, *Exp Fluids*, 2002, **33**, pp 181-187.
26. DALZIEL, S.B., HUGHES, G.O. and SUTHERLAND, B.R. Whole-field density measurements by synthetic schlieren, *Exp Fluids*, 2000, **28**, pp 322-335.
27. RAGUNATH, S., MEE, D.J. ROESGEN, T. and JACOBS, P.A. Background oriented Schlieren for visualization in hypersonic impulse facilities, in: Proc 25th Int Symp Shock Waves, 2005, pp 865-870, Indian Institute of Science, Bangalore, India.
28. BONE, D.J., BACHOR, H.A. and SANDEMAN, R.J. Fringe-pattern analysis using a 2-D Fourier transform. *Appl Opt*, 1986, **25**, (10), pp 1653-1660.
29. BONE, D.J. Fourier fringe analysis – the two-dimensional phase unwrapping problem. *Appl Opt*, 1991, **30**, (25), pp 3627-3632.
30. BABINSKY, H. and TAKAYAMA, K. Quantitative holographic interferometry of shock-wave flows using Fourier transform fringe analysis. In: Proc 20th Int Symp Shock Waves, Pasadena, USA, July 1995, World Scientific Press, pp 1599-1604.
31. BISHOP, A.I. Spectrally Selective Holographic Interferometry Techniques for Flow Diagnostics, PhD Dissertation, 2001, The University of Queensland, Brisbane, Australia.
32. VEST, C.M. *Holographic Interferometry*, 1979, John Wiley and Sons Inc, 1979.
33. TAKAYAMA, K. Application of holographic interferometry to shock wave research. Proc SPIE, 1983, **398**, pp 174-180.
34. HOUWING, A.F.P., TAKAYAMA, K., JIANG, Z., SUN, M., YADA, K. and MITOBE, H. Interferometric measurement of density in nonstationary shock wave reflection flow and comparison with CFD, *Shock Waves*, 2005, **14**, (1-2), pp 11-19.
35. SANDERSON, S. Shock Wave Interaction in Hypersonic Flow, PhD Dissertation, California Institute of Technology, 1995.
36. NONAKA, S., TAKAYAMA, K. Density measurement over a sphere in ballistic range, AIAA Paper 2000-0837, Reno, 2000.
37. GUO, L.D., ZHOU, Z.F., YANG, H. and ZHANG, L. Holographic interference measurement of the hypersonic flow field, *Optical Engineering*, 2005, **44**, (1), Art. No 015603.
38. MCINTYRE, T.J., EICHMANN, T.N., HAJEK, K. and KOVACHEVICH, A. Visualisation and measurement of flow on the inlet of an upstream injected supersonic-combustion ramjet, In: Proc Fourth Australian Conference on Laser Diagnostics in Fluid Mechanics and Combustion, 2005, McLaren Vale, SA, Australia, The University of Adelaide.
39. MCINTYRE, T.J., HAJEK, K.M., EICHMANN, T.N. and KOVACHEVICH, A.L. Interferometric visualization of fuel concentrations on the intake of a supersonic combustion ramjet engine. In: Proc 12th Int Symp Flow Visualization, Göttingen, Germany.
40. KASTELL, D., CARL, M. and EITELBERG, G. Phase step holographic interferometry applied to hypervelocity non-equilibrium cylinder flow, *Exp Fluids*, 1996, **22**, pp 57-66.
41. SURGET, J. and DUNET, G. Multipass holographic interferometer for the high enthalpy hypersonic wind tunnel F4, in: *Proc. of the NATO Advanced Research Workshop New Trends in Instrumentation for Hypersonic Research*, pp 135-151, Kluwer, Dordrecht, 1993.
42. HOUWING, A.F.P., TAKAYAMA, K., JIANG, Z., HASHIMOTO, T., KOREMOTO, K., MITOBE, H. and GASTON, M.J. Abel inversion of axially-symmetric shock wave flows, *Shock Waves*, 2005, **14**, (1-2), pp 21-28.
43. MORTON, J. Tomographic Imaging of Supersonic Flows, PhD Thesis, 1995, Department of Physics, Faculty of Science, Australian National University, Canberra, Australia.
44. FALETIC, R. Tomographic Reconstruction of Shock Layer Flows, PhD Thesis, 2005, Department of Physics, Faculty of Science, Australian National University, Canberra, Australia.
45. THORNE, A.P. *Spectrophysics*, Chapman and Hall, London, 1988.
46. MCINTYRE, T.J., WEGENER, M.J., BISHOP, A.I. and RUBINSZTEIN-DUNLOP, H. Simultaneous two-wavelength holographic interferometry in a super-orbital expansion tube facility, *Appl Opt*, 1997, **36**, (31), pp 8128-8134.
47. MCINTYRE, T.J., BISHOP, A.I., THOMAS, A.M., SASOH, A. and RUBINSZTEIN-DUNLOP, H. Ionizing Nitrogen and Air Flows in a Superorbital Expansion Tube, *AIAA J.* 2000, **38**, (9), pp 1685-1691.
48. MCINTYRE, T.J., BISHOP, A.I., RUBINSZTEIN-DUNLOP, H. and GNOFFO, P.A. Experimental and numerical studies of ionizing flow in a super-orbital expansion tube, *AIAA J.* 2003, **41**, (11), pp 2157-2161.
49. MCINTYRE, T.J., BISHOP, A.I. and RUBINSZTEIN-DUNLOP, H. Two-wavelength holographic interferometry as a diagnostic tool for ionising flows, In: Proc 9th Int Symp Flow Visualization, August, 2000, Edinburgh, Scotland, UK.
50. MEASURES, R.M. Spectral line interferometry: a proposed means of selectively measuring the change in the density of a specific atomic population, *Appl Opt*, 1970, **9**, (3), pp 737-741.
51. BISHOP, A.I., LITTLETON, B.N., MCINTYRE, T.J. and RUBINSZTEIN-DUNLOP, H. Near-resonant holographic interferometry of hypersonic flow. *Shock Waves*, 2001, **11**, (1), pp 23-29.

52. MCINTYRE, T.J., BISHOP, A.I., EICHMANN, T.N. and RUBINSZTEIN-DUNLOP, H. Enhanced flow visualisation using near-resonant holographic interferometry, *Appl Opt*, 2003, **42**, (22), pp 4445-4451.
53. MCINTYRE, T.J., LOUREL, I., EICHMANN, T.N., MORGAN, R.G., JACOBS, P.A. and BISHOP, A.I. An experimental expansion tube study of the flow over a toroidal ballute, *J Spacecraft and Rockets*, 2004, **41**, (5), pp 716-725.
54. EICHMANN, T.N. An Experimental Investigation of Shock Shapes and Shock Stand-offs in a Super-Orbital Facility, Masters Thesis, 2004, The University of Queensland, Brisbane, Australia.
55. DESSE, J.-M., ABLE, F. and TRIBILLON J.-L. Real-time color holographic interferometry, *Appl Opt*, 2002, **41**, (25), pp 5326-5333.
56. BARNHART, D.H., KOEK, W.D., JUCHEM, T., HAMPP, N., COUPLAND, J.M. and HALLIWELL, N.A. Bacteriorhodopsin as a high-resolution, high-capacity buffer for digital holographic measurements, *Meas Science and Tech.*, 2004, **15**, (4), pp 639-646.
57. DEMOLI, N., VUKICEVIC, D. and TORZYNSKI, M. Dynamic digital holographic interferometry with three wavelengths, *Optics Express*, 2003, **11**, (7), pp 767-774.
58. HRUSCHKA, R. and KLEINE, H. Visualization of three-dimensional flows, In: Proc 25th Int Symp Shock Waves; Bangalore, India, pp 173-178, 2005
59. ECKBRETH, A.C., *Laser Diagnostics for Combustion Temperature and Species*, 2nd ed, Gordon and Breach, 1996.
60. PALMA, P.C., DANEHY, P.M. and HOUWING, A.F.P. Fluorescence imaging of rotational and vibrational temperature in a shock tunnel nozzle flow, *AIAA J*, 2003, **41**, (9), pp 1722-1732.
61. HANSON, R.K. and SEITZMAN, J.M. Planar fluorescence imaging in gases, In: *Handbook of Flow Visualization*, 1989, Hemisphere Pub Corp, pp 219-232.
62. HANSON, R.K. Planar Laser-Induced Fluorescence Imaging, *J Quant Spectrosc and Radiat Trans*, 1988, **40**, pp 343-362.
63. SEITZMAN, J.M. and HANSON, R.K. Fluorescence Imaging in Gases, *Instrumentation for Flows with Combustion*, 1993, pp 445-446.
64. DOHERTY, P.M. and CROSLY, D.R. Polarisation of laser-induced fluorescence of OH in an atmospheric pressure flame, *Appl Opt*, 1982, **23**, pp 713-721.
65. EBATA, T., ANEZAKI, Y., FUJII, M., MIKAMI, N. and ITO, M. Rotational energy transfer in NO ($A^2\Sigma^+$, $v = 0$ and 1) studied by two-color double-resonance spectroscopy, *J Chem Phys*, 1984, **84**, pp 151-157.
66. BERG, J.O. and SHACKLEFORD, W.L. Rotational redistribution effect on saturated laser-induced fluorescence, *Appl Opt*, 1979, **18**, (13), pp 2093-2094.
67. STEPHENSON, J.C. Vibrational-relaxation of NO X $^2\Pi(v = 1)$ in the temperature range 100-300K, *J Chem Phys*, 1974, **60**, pp 4289-4294.
68. PALMA, P.C., MCINTYRE, T.J. and HOUWING, A.F.P. Thermometry in shock tunnel flows using a Raman-shifted tunable excimer laser, *Shock Waves*, 1998, **8**, (5), pp 275-284.
69. GREENSTEIN, H. and BATES, J., C.W. Line-width and tuning effects in resonant excitation, *J Opt Soc Am*, 1975, **65**, (1), pp 33-40.
70. DAILY, J.W. Use of rate equations to describe laser excitation in flames. *Appl Opt*, 1977, **16**, (8), pp 2322-2327.
71. YARIV, A. *Quantum Electronics*, 3rd ed, Wiley & Sons, New York, 1988.
72. PIEPMEIER, E.H. Theory of laser saturated atomic resonance fluorescence, *Spectrochimica Acta Part B*, 1972, **27**, (10), pp 431-443.
73. ALTKORN, R. and ZARE, R.N. Effects of saturation on laser-induced fluorescence measurements of population and polarisation, *Annual Review of Physical Chemistry*, 1984, **35**, pp 265-289.
74. DAILY, J.W. Saturation effects in laser induced fluorescence spectroscopy, *Appl Opt*, 1977, **16**, (3), pp 568-571.
75. PAUL, P.H., GRAY, J.A., DURANT, J.L., JR and THOMAN, J.W., JR Collisional quenching corrections for laser-induced fluorescence measurements of NO $A^2\Sigma^+$, *AIAA J*, 1994, **32**, pp 1670-1675.
76. FOX, J.S., O'BYRNE, S., HOUWING, A.F.P., PAPPINNIEMI, A., DANEHY, P.M. and MUDFORD, N.R. Fluorescence Visualization of Hypersonic Flow Establishment over a Blunt Fin, *AIAA J*, 2001, **39**, (7), pp 1329-1337.
77. PALMER, J.L., HOUWING, A.F.P., THURBER, M.C., WEHE, S.D. and HANSON, R.K. PLIF imaging of transient shock phenomena in hypersonic flows, In: 18th Aerospace Ground Testing Conference, June, 1994, AIAA-1994-2642.
78. O'BYRNE, S.B., HOUWING, A.F.P. and DANEHY, P.M. Establishment of the near-wake flow of a cone and wedge in a transient hypersonic freestream, In: Proc 22nd Int Symp Shock Waves, July 1999, pp 1583-1588.
79. CLEMENS, N.T. An experimental investigation of scalar mixing in supersonic turbulent shear layers, PhD Dissertation, Department of Mechanical Engineering, Stanford University, 1991.
80. McMILLIN, B.K. Instantaneous Two-Line PLIF Temperature Imaging of Nitric Oxide in Supersonic Mixing and Combustion Flow Fields, PhD Dissertation, Department of Mechanical Engineering, Stanford University, 1993.
81. FOX, J.S., HOUWING, A.F.P., DANEHY, P.M., GASTON, M.J., MUDFORD, N.R. and GAI, S.L. Mole-Fraction-Sensitive Imaging of Hypermixing Shear Layers, *J Propulsion and Power*, 2001, **7**, (2), pp 284-292.
82. GASTON, M.J., HOUWING, A.F.P., MUDFORD, N.R., DANEHY, P.M. and FOX, J.S. Fluorescence imaging of mixing flowfields and comparisons with computational fluid dynamic simulations, *Shock Waves*, 2002, **12**, (2), pp 99-110.
83. HOUWING, A.F.P., BISHOP, A., GASTON, M.J., FOX, J.S., DANEHY, P.M. and MUDFORD, N.R. Simulated-fuel-jet/shock-wave interaction, In: Proc 23rd Int Symp Shock Waves, July 2001, pp 1074-1080.
84. ROSSMANN, T., MUNGAL, M.G. and HANSON, R.K. Nitric-oxide planar laser-induced fluorescence applied to low-pressure hypersonic flow fields for the imaging of mixture fraction, *Appl Optics*, 2003, **42**, (33), pp 6682-6695.
85. MCINTYRE, T.J., HOUWING, A.F.P., PALMA, P., RABBATH, P. and FOX, J.S. Imaging of combustion in a supersonic-combustion ramjet, *J Propulsion and Power*, 1996, **13**, (3), pp 388-394.
86. O'BYRNE, S., STOTZ, I., NEELY, A., BOYCE, R. and MUDFORD, N. OH PLIF Imaging of Supersonic Combustion Using Cavity Injection, Paper AIAA-2005-3357, AIAA/CIRA 13th International Space Planes and Hypersonics Systems and Technologies Conference, Capua, Italy, 16-20 May 2005.
87. McMILLIN, B.K., PALMER, J.L. and HANSON, R.K. Temporally-resolved two-line fluorescence imaging of NO temperature in a transverse jet in a supersonic crossflow, *Appl Opt*, 1993, **32**, pp 7532-7545.
88. PALMER, J.L. and HANSON, R.K. Temperature imaging in a reacting, supersonic free jet using two-line OH fluorescence, *Appl Opt*, 1996, **35**, (3), pp 485-499.
89. PALMER, J.L., McMILLIN, B.K. and HANSON, R.K. Multi-line fluorescence imaging of the rotational temperature field in a shock tunnel, *Appl Phys B*, 1996, **63**, (167), pp 167-178.
90. RUYTEN, W.M. Comparison of calculated and measured temperature fields in the AEDC Impulse Facility, AIAA-1996-2237, 1996.
91. BECK, W.H., EITELBERG, G., TRINKS, O. and WOLLENHAUPT M. Testing methodologies in the DLR High Enthalpy Shock Tunnel HEG, AIAA-1998-2770, 1998.
92. ROBERTS, W.L., ALLEN, M.G., HOWARD, R.P., WILSON, G.J. and TRUCCO, R. Measurement and prediction of nitric oxide concentration in the HYPULSE Expansion Tube Facility, AIAA 94-2644, 1994.
93. SUTTON, D.S., HOUWING, A.F.P., PALMA, P.C. and SANDEMAN, R.J. Vibrational temperature measurements in a shock layer using laser induced predissociation fluorescence, *Shock Waves*, 1993, **3**, (2), pp 141-148.
94. PALMA, P.C., HOUWING, A.F.P. and SANDEMAN, R.J. Absolute intensity measurements of impurity emissions in a shock tunnel and their consequences for laser induced fluorescence experiments, *Shock Waves*, 1993, **3**, (1), pp 49-53.
95. McDANIEL, J.C., HILLER, B. and HANSON, R.K. Simultaneous multiple-point velocity measurements using laser induced iodine fluorescence, *Opt Lett*, 1983, **8**, (1), pp 51-53.
96. DANEHY, P.M., MERE, P., GASTON, M.J., O'BYRNE, S., PALMA, P.C. and HOUWING, A.F.P. Fluorescence velocimetry of the hypersonic, separated flow over a cone, *AIAA J*, 2001, **39**, (7), pp 1320-1328.
97. MILES, R.B., LEMPERT, W. and ZHANG, B. Turbulent structure measurements by RELIEF flow tagging, *Fluid Dynamics Research* 1991, **8**, pp 9-17.
98. MILES, R.B., GRINSTEAD, J., KOHL, R.H. and DISKIN, G. The RELIEF flow tagging technique and its application in engine testing facilities and for helium-air mixing studies, *Meas Sci Techno*, 2000, **11**, pp 1-10.
99. DANEHY, P.M., O'BYRNE, S., HOUWING, A.F.P., FOX, J. and SMITH, D.R. Flow-Tagging Velocimetry for Hypersonic Flows Using Fluorescence of Nitric Oxide. *AIAA J*, 2003, **41**, (2), pp 263-271.
100. O'BYRNE, S., DANEHY, P.M., HOUWING, A.F.P., MALLINSON, S.G. and PALMA, P.C. Temperature and velocity measurements in a hypersonic boundary layer. In: Proc 23rd Int Symp Shock Waves, 2001 Fort Worth, Texas, USA.
101. BARKER, P., BISHOP, A. and RUBINSZTEIN-DUNLOP, H. Supersonic velocimetry in a shock tube using laser enhanced ionisation and planar laser induced fluorescence, *Appl Phys B*, 1997, **64**, pp 369-376.
102. JOHN, C.T. and TURK, G.C. *Laser-Enhanced Ionization Spectroscopy*, John Wiley, New York, 1996.
103. LITTLETON, B.N., BISHOP, A.I., MCINTYRE, T.J., BARKER, P.F. and RUBINSZTEIN-DUNLOP, H. Flow tagging velocimetry in a superorbital expansion tube. In: Proc 21st Int Symp Shock Waves, 1997, Great Keppel Island, Australia, pp 511-515.